universität wien

DIPLOMARBEIT

Titel der Diplomarbeit

Study of the function of the histone methyltransferase EZH2 in human cancers

Verfasserin

Renner Magdalena

angestrebter akademischer Grad

Magistra der Naturwissenschaften (Mag.rer.nat.)

Wien, 30.01.2012

Studienkennzahl lt. Studienblatt:	A 490
Studienrichtung lt. Studienblatt:	Diplomstudium Molekulare Biologie
Betreuer:	Ao Univ.-Prof. Dr. Christian Seiser

The Diploma Thesis research was carried out in the Laboratory of Davide Gianni, Department Lead Discovery at Boehringer Ingelheim GmbH & CoKG Vienna, Austria

Danksagung

Ich möchte an dieser Stelle allen danken, die mich auf meinem Weg durchs Studium unterstützt und begleitet haben!

Ein besonderer Dank gilt meiner Familie, die mir das Studium ermöglicht hat und immer voller Vertrauen hinter mir steht.

Außerdem möchte ich meinem Betreuer, Davide Gianni danken, für die lehrreiche Zeit in seinem Labor, die interessanten Diskussionen und vermittelte Motivation. Mille Grazie!
Danke auch an meine Kolleginnen und Kollegen im Labor, für die schöne Zeit, die wir gemeinsam hatten.

Meinen Freundinnen und Freunden möchte ich auch ganz herzlich danken für all die tollen Erlebnisse die hinter, und noch vor uns liegen.

Und danke Benjamin, dass du einfach immer für mich da bist!

Table of Contents

Table of Contents 4

ABSTRACT 7

ZUSAMMENFASSUNG 8

INTRODUCTION 9

Epigenetic gene regulation 9

A key player in differentiation and development: the PRC2 11

The EZH2 homolog EZH1 13

Regulation of PRC2 14

Targets of the Polycomb Group Proteins 16

The role of EZH2 in stem cell maintenance and differentiation 17

A stem cell link to cancer 17

The role of EZH2 in cancer 18

THESIS RATIONALE 22

ABBREVIATIONS 23

MATERIALS AND METHODS 25

General Cell Culture Work 25

Cell Lines 25

Passaging of cells 25

Determination of cell number and viability 26

Freezing of cells 26

Thawing of cells 27

shRNA Experiments 27

Experiment Summary 28

Determination of optimal puromycin concentrations 29
Lentiviral transduction 30
Cell Proliferation Assays 31
Measurement of confluence with the Genetix CloneSelect™ Imager (CSI) 31
2 D Alamar Blue assays measuring metabolism 33
Soft agar colony formation assay 33
Determination of Protein knockdown and Biomarker status 34
Preparation of whole cell lysates 34
Western Blot 35
siRNA experiments 38
Reverse transcription quantitative PCR (RT q-PCR) 39
RESULTS 42
EZH2 is overexpressed in human cancer tissues 42
EZH2 is overexpressed in a broad panel of human cancer cell lines 43
Verification of data derived from the TANGO database by Western blot 45
Study of the role of EZH2 in human cancer cell proliferation 45
Knockdown of EZH2 by siRNA 45
Knockdown of EZH2 by shRNA 47
Effect of different cell densities on cell proliferation differences 49
Effect of EZH2 knockdown in cell lines with an EZH2 point mutation 52
Reduced proliferation of EZH2 amplified cells 54
Reduced proliferation in UTX deleted MiaPaca-2 cells 55
Effect of EZH2 knockdown in prostate cancer cells 57
Androgen insensitive prostate cancer cells: PC3 57
Androgen sensitive prostate cancer cells: LNCaP.FGC 58

EZH2 knockdown reduces anchorage independent growth 59

Repression of target genes by EZH2 knockdown 61

DISCUSSION 63

SUMMARY 68

REFERENCES 69

List of figures 73

List of tables 74

Curriculum Vitae 76

ABSTRACT

EZH2, the catalytic component of polycomb repressive complex 2 (PRC2), is responsible for the mono-, di- and trimethylation of histone H3 on lysine 27 (H3K27). H3K27 trimethylation marks genes, many of which are involved in development and differentiation, for epigenetic silencing. EZH2 is normally not expressed in differentiated cells and it was found to be highly overexpressed, amplified or mutated in multiple tumor types, including melanoma, breast and prostate cancers. The level of EZH2 overexpression has been correlated with poor clinical prognosis indicating that EZH2 is a highly relevant protein target for cancer therapeutics.

To study the effect of EZH2 on cancer cell proliferation, we knocked down the expression of this enzyme in various cancer cell lines by lentiviral introduction of short hairpin RNA. The stable knockdown of the protein enabled us to follow cell proliferation by colony formation and/or metabolic-based cell proliferation assays for up to 21 days after viral transduction. In parallel, we tested the effect of the prolonged EZH2 knockdown on the methylation status of total H3K27 by Western blot. We found that EZH2 knockdown strongly reduced cell proliferation in several cell lines from different tumor origin as compared to a non targeting control shRNA. This effect on cell proliferation was accompanied by a reduction of global trimethylation of H3K27. The extent of proliferation reduction nevertheless seemed to be dependent on the different cell lines and the underlying EZH2 aberrations such as overexpression, gene amplification, EZH2 point mutation or deletion of the EZH2 antagonist UTX.

Furthermore, since EZH2 is involved in the repression of a multitude of developmentally important genes (including many tumor suppressor proteins), we selected a panel of published EZH2 target genes and were testing the change of mRNA expression levels upon knockdown of EZH2 by RT q-PCR.

We verified EZH2 as a promising target in cancer treatment and more closely defined the patient population which could benefit of treatment by an EZH2 inhibitor.

ZUSAMMENFASSUNG

EZH2, die katalytische Untereinheit des Polycomb repressive complex 2 (PRC2), ist für die Mono-, Di- und Trimethylierung von Histon H3 an Lysin 27 (H3K27) verantwortlich. Diese Modifikation markiert Gene, welche für Differenzierung und Entwicklung wichtig sind, für epigenetische Stilllegung. EZH2 wird normalerweise in differenzierten Zellen nicht exprimiert. In vielen Tumortypen wie Brust-und Prostatakrebs, sowie Melanomen ist es jedoch überexprimiert, amplifiziert oder mutiert. EZH2 Expressionslevel wurden in vielen Studien mit schlechter klinischer Prognose assoziiert, weshalb EZH2 ein hochrelevantes Ziel für die Therapie aggressiver Tumore ist.

Um den Effekt von EZH2 auf die Proliferation von Krebszellen zu testen, haben wir die Expression des Enzyms in verschiedenen Krebszelllinien mittels lentiviral eingebrachter shRNA gehemmt. Der stabile Knockdown ermöglichte uns, die Zellproliferation mittels Konfluenz- und/oder Metabolismus- basierten Zellproliferations-Assays für bis zu 21 Tage nach der Transduktion zu verfolgen. Gleichzeitig konnten wir den globalen Methylierungszustand von H3K27 mittels Western Blot überprüfen. Der Knockdown von EZH2 reduzierte das Wachstum von Tumorzellen verschiedenen Ursprungs im Vergleich mit einer Kontroll-shRNA. Dieser Effekt auf die Zellproliferation wurde von einer Reduktion der globalen H3K27 Trimethylierung begleitet. Das Ausmaß der Wachstumsreduktion war jedoch abhängig vom Zelltyp und der zugrundeliegenden Deregulation von EZH2 wie Überexpression, Punktmutation, Gen-Amplifikation und Deletion des EZH2 Gegenspielers UTX.

Da EZH2 für die Regulation einer Vielzahl von Entwicklungsgenen beteiligt ist (darunter viele Tumorsuppressor-Proteine), haben wir eine Reihe publizierter EZH2-Zielgene ausgewählt und die Veränderung deren mRNA Expressions-Level nach Knockdown von EZH2 mittels quantitativer reversen Transkriptase PCR getestet.

Wir konnten zeigen, dass EZH2 ein vielversprechendes Ziel in der Krebstherapie ist und konnten außerdem die Patientenpopulation, die womöglich von on einem EZH2-Inhibitor profitiert, genauer eingrenzen.

INTRODUCTION

Epigenetic gene regulation

The human body contains at least 200 different types of cells, which share an identical genome. The response of these cells to extra- or intracellular signals is dependent on their special lineage "identity" [1]. The lineage identity of each cell in a multi-cellular organism is determined by the unique gene-expression pattern of that cell type. This must be remembered and passed on to daughter cells by epigenetic mechanisms, which are heritable changes that do not involve changes in DNA sequence [2]. The epigenetic state of cells represents the sum of developmental and physiological influences acting on a cell and thereby provides an important interface in between the genome and the environment [3].

The three main epigenetic mechanisms are DNA methylation, chromatin remodeling and micro RNA (miRNA) regulation [4].

DNA is packaged into the nucleus in the form of Chromatin which is a complex of DNA and associated proteins [5]. The chromatin is organized into nucleosomes, which are comprised of a histone octamer (a histone H3-H4 tetramer and two H2A-H2B dimers) around which 147 base pairs of DNA are wrapped in 1.75 superhelical turns [6, 7]. The nucleosomes are separated by 10-16 base pairs (bp) of linker DNA and this "beads on a string" arrangement constitutes a chromatin fiber of about 10nm in diameter [8]. A further compaction of chromatin is promoted by the Histone H1 [9].

Histones are very dynamic proteins which physically support DNA and are involved in regulating transcription, repair and replication [4]. They share a structural motif, called the "histone fold", formed by three α-helices connected by loops. Each of the core histones has a long, highly conserved N-terminal amino acid "tail" extending outwards from the DNA-histone core [5]. These histone tails do not contribute to the structure of individual nucleosomes or their stability, but play an important role in folding the nucleosome arrays into higher order chromatin structure [8]. The N-terminal histone tails can be post-translationally modified by acetylation and methylation of lysines (K)

and arginines (R), phosphorylation of serine (S) and threonines (T), ubiquitination, sumoylation and biotinylation of lysines as well as ADP ribosylation [8]. Modification of histone tails is dependent on two antagonizing groups of enzymes, namely “writers” and “erasers”. Such enzymes can transfer or remove histone marks, respectively. The So-called “readers” are able to ”read” these modifications and recruit other protein complexes thus triggering cellular events such as activation or repression of gene transcription [7]. Among the diverse modifications, histone methylations at lysine and arginine residues are relatively stable. The epigenetic information can thus be remembered through several cell divisions. Therefore, enzymes that catalyze the methylation reaction play critical roles in development and pathological processes [10].

High resolution profiling of histone methylations in the human genome revealed that monomethylations of at least H3K9, H3K27, and H3K79 are associated with gene activation, whereas the trimethylation is linked to repression [6]

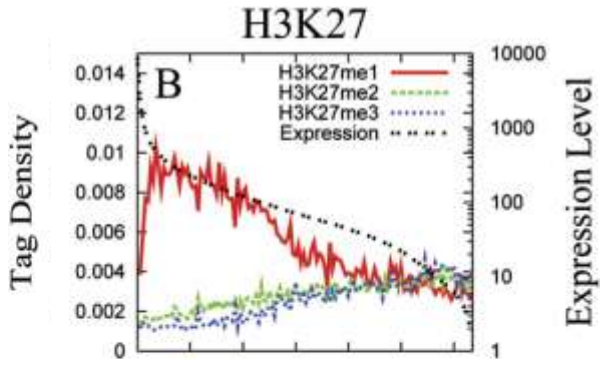

Figure 1. Modified from Barski et al. 2007. Correlation of Histone Methylations in Transcribed Regions with Expression Levels. The group divided 12 726 genes in different activity groups and plotted the gene expression levels against their average modification levels in their transcribed regions. “*Genes were separated into groups of 100 genes based on their expression levels from high to low (left to right on the x axis). The right y axis indicates the expression level of each group. The left y axis indicates the histone methylation level that was derived by summing up all the detected ChIP Sequencing tags within the entire transcribed gene-body regions and normalized to the total base pair number of the 100 genes*” **[10]**.

Gene silencing at the chromatin level is crucial for the life of eukaryotic organisms and is especially important in orchestrating key biological processes such as differentiation, imprinting and silencing of large chromosomal domains such as the X chromosome, over the life span of female mammals [11]. Epigenetic modifications are controlled by

complex enzymatic machineries which include specific histone methylases (HKMTs) and demethylases (HKDMs). Deregulation of these machineries could alter chromatin configuration and disrupt normal transcriptional programs, both of which are features of cancer cells [12].

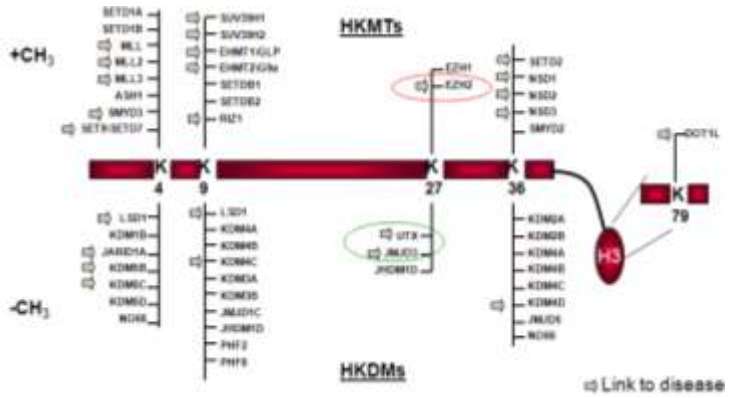

Figure 2. Modified from poster presented at AACR 2010. Readers and writers adding and removing methyl-groups at lysines of Histone H3. Histone lysine methyl transferases (HKMTs) are adding methyl groups and Histone lysine demethylases (HKDMs) are removing lysines at different lysines of histone H3. Histone H3 lysine 27 (H3K27) is modified by a relatively low amount of proteins which makes it a well suited target for research. All proteins marked with an arrow are involved in various diseases such as cancer.

Figure 2 shows several writers HKMTs and erasers HKDMs acting at various lysines of the N-terminal tail of histone H3. Many of those enzymes have been reported to be involved in the pathogenesis of many diseases including cancer and are therefore interesting targets in drug discovery. As shown in Figure 2, Histone 3 Lysine 27 (H3K27) however is modified by only a relatively small amount of enzymes; the methyltransferases EZH2 and EZH1, and the demethylases UTX and JMJD3.

A key player in differentiation and development: the PRC2

Analysis of genetic data in *Drosophila melanogaster* showed that both repressed and active gene expression states tend to be inherited through successive cell cycles and throughout development. Polycomb group (PcG) and Trithorax group (TrxG) proteins were identified as factors that maintain silent and active transcriptional states of homeotic (Hox) genes [7]. Subsequent genome-wide analysis of PcG complexes in mouse

and human embryonic stem cells (ESCs) revealed that they also bind to genes encoding developmental regulators, thus demonstrating that PcG mechanisms discovered in *Drosophila* are conserved throughout evolution. [7]. The PRC2 is involved in repression of differentiation genes and transcription factors, X-chromosome inactivation, stem cell maintenance and cancer [13].

PcG proteins form two functionally and biochemically distinct multimeric Polycomb repressive complexes (PRCs), called PRC1 and PRC2 [6].

Fly and human PRC2 have quite similar core subunit compositions [13] (Figure 3). The core components of PCR2 are suppressor of zeste-12 (SUZ-12), embryonic ectoderm development (EED), and enhancer of zeste homolog 2 (EZH2) [14]. Human EZH2 was isolated by Laible and colleagues in 1997 [15]. EZH2 is responsible for the specific methylation of Lysine 27 on histone H3. The H3K27 methyltransferase contains the signature SET domain (Su(var)39, E(z), Trithorax) which is the methyltransferase active site [9, 17]. Both the SET domain and the adjacent cysteine-rich CXC domain are required for histone methyltransferase activity [13](Figure 3). The enzyme can add up to 3 methyl groups to the ε-amino group of H3K27. The repressive tri-methylated form of H3K27 is regarded as the main form that conveys biological function in vivo [13]. However, to act as an active methyltransferase enzyme, EZH2 needs to be complexed with the non catalytic proteins EED and SUZ-12, [13, 16, 17]. EED contains seven WD40 repeats at its C-terminus and functions as a scaffold protein by physically linking EZH2 and histone H3 substrates [18]. SUZ12 is required for the integrity of the PRC2 and for the stabilization of EZH2 at the protein level [19]. RbAp46/48 function as histone binding proteins [16]. PRC2 enzyme activity or its recruitment to target sites can be influenced by association of the protein PHF1 which is not part of the core complex [13]. The core components of PRC2 are evolutionary conserved in plants and *C. elegans* [20].

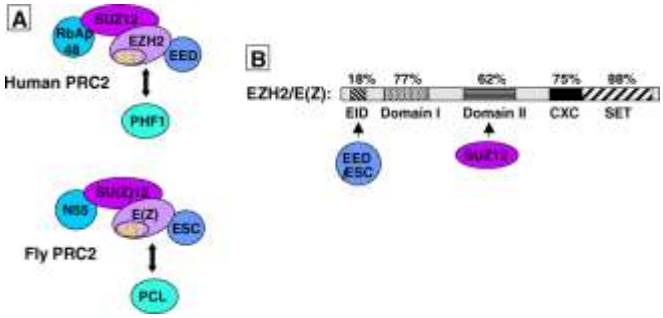

Figure 3. Adapted from Simon et al. 2008. "*Composition of PRC2 and domain organization of EZH2. (A)* *The four core subunits of human PRC2 are EZH2, EED, SUZ12 and RbAp48 and the corresponding homologous subunits in fly PRC2 are E(Z), ESC, SU(Z)12 and NURF55. EZH2/E(Z) is the catalytic subunit that contains a SET domain. PHF1/PCL is another Polycomb protein that can associate with PRC2 to influence its activity and/or targeting.* *(B)*** *Five functional domains in EZH2/E(Z) are depicted, with % identities between the human and fly versions indicated. The SET domain houses the histone methyltransferase active site and the CXC domain also contributes to activity. Robust methyltransferase requires EZH2 assembly with both EED/ESC and SUZ12, and domains required for binding these non-catalytic subunits are indicated.*" **[13]**

The **PRC1** contains more than 10 subunits including the oncoprotein BMI-1 and the HPC proteins (CBX2, CBX4, CBX7, CBX8), HPH1-3, RING1-2, and SCML [1]. There is a significant overlap of promoters bound by PRC1 and PRC2 which are also tri-methylated on H3K27 [1]. The complex can bind to the trimethylated form of H3K27 via its chromodomain, mediating ubiquitination of H2AK119 to maintain gene repression [14]. The presence of PRC1 at target gene promoters seems to block elongation by Polymerase II (POLII) [21]. Furthermore PRC1 can condense chromatin in the absence of histone tails and prevents the ATP-dependent remodeling activity of Swi/Snf in vitro [22].

The EZH2 homolog EZH1

EZH1 is a well conserved homolog of EZH2 and was the first mammalian homolog of *Drosophila* Ez to be cloned by Abel and colleagues in 1996 [23]. EZH1 is found mainly in non-proliferative adult organs, while EZH2 expression is closely associated with proliferating cells [22].

EZH1 was shown to be a member of an alternative Polycomb repressive complex 2 together with EED, SUZ12 and RbAP46/48 [22, 24]. EZH1 acts as a histone

methyltransferase on H3K27 in the context of a nucleosome octamer, but in vitro methylation experiments showed 20fold weaker methylation activity as compared to EZH2 [22]. Remarkably, the repressive effect of EZH1 on chromatin may depend on its ability to compact chromatin independently of histone methylation and previous histone modifications [22].

Shen et al 2008 reported that in EZH2 $^{-/-}$ embryonic stem cells a subset of developmental genes showed preserved H3K27me3 and robust H3K27me1 despite global loss of di- and trimethylation of H3K27. The H3K27 methyltransferase EZH1 can help to maintain ESCs in an undifferentiated state, nevertheless differentiation is profoundly disturbed in the absence of EZH2. Knockdown of EZH1 by RNAi in wild type ESCs did not affect the expression of PcG target genes, supporting EZH2 as the major histone methyltransferase controlling the methylation state of H3K27. These data imply non-redundant roles of the two methyl transferases during epigenetic cell fate establishment [24].

An in vivo study by Ezhkova and colleagues nevertheless reported compensatory methylase activities of EZH1 and EZH2 in conditional knockout mouse skin. Although ESCs are dependent on EZH2, skin progenitors can maintain stemness and differentiation programs for a limited period of time with either low or no PcG silencing [25]. The most striking abnormality found in Ezh1/2-null skin was the progressive and complete loss of regenerative potential of the hair follicle lineage. EZH1/2 double knockout skin progenitors upregulated non-skin PcG-regulated genes to a much less extent compared to their natural lineages, without rerouting already established skin fates. These data highlight the importance of tissue-specific transcription factors in fully activating PcG target genes [25].

Regulation of PRC2

In Drosophila the PRC2 complex is recruited to target genes by so called Polycomb response elements (PREs). However in mammals such sequences have yet to be precisely defined [13]. The transcriptional regulator YY1 was found to recruit EZH2 to

specific loci in muscle cells [26]. In nasopharyngeal carcinoma it was reported that Snail recruits EZH2 to the E-cadherin promoter, by bridging the interaction to EZH2 associated HDAC1 and HDAC2; in addition, disruption of HDAC function also abrogates the function of PRC2 [27]. Furthermore, Bracken and colleagues showed that EZH2 is regulated by the pRB-E2F pathway, one of the most frequently deregulated pathways in cancer [28]. High EZH2 and EED expression is strongly increased in proliferating cells as compared to non-proliferating differentiated cells and the expression of EZH2 and EED can be re-induced in starved cells stimulated to proliferate [28]. Temporal downregulation of PRC2 components along with a decrease in repressive H3K27me3 in injured murine skin epithelium leads to re-expression of repair genes and wound repair [29].

EZH2 was shown to be negatively regulated by micro RNA (miR)-101 in prostate cancer [30-32] and pancreas carcinoma [32, 33]. It was found that the expression of EZH2 was higher in malignant than in benign pancreatic cancers, with an inverse correlation to miR-101 expression [33]. In prostate carcinomas, miR-101 is regulated by androgen receptor and HIF-1α/HIF-1β [32].

EZH2 is highly phosphorylated and thereby can assemble and integrate distinct signals to directly convert them into chromatin modifications. Phosphorylation of EZH2 at different sites affects interactions with chromatin, non-coding RNAs or other members of the PRC2 [34]. Kaneko and colleagues verified the interaction of EZH2 with the non coding RNAs HOTAIR and Xist [35]. HOTAIR targets PRC2 to some of its chromatin targets and by also binding the LSD1/CoREST/REST complex serves as a platform for coupled H3K27 methylation and lysine 4 demethylation [36]. Recruitment of EZH2 to the X-chromosome by the ncRNA RepA is involved in initiation and spread of X-chromosome inactivation [37].

Bracken and colleagues found that the promoters of the PRC1 components BMI-1 and CBX8 gene loci are bound by SUZ-12 and CBX8 and are associated with increased H3K27me3. Depletion of PRC1 or PRC2 members by siRNA increased the expression of BMI-1 and CBX8 indicating autoregulation of PcG components expression [1].

Targets of the Polycomb Group Proteins

Several studies identified global PcG binding sites in human embryonic fibroblasts [1], human embryonic stem cells [38], or murine embryonic stem cells [39], reviewed by Leonie Ringrose in 2007 [40].

All three studies report occupation of PcG components and the H3K27 trimethylation mark on genes important for development and differentiation, the most prevalent proteins being transcription factors. Furthermore, PcG target genes in undifferentiated cells have the potential to become activated upon cell differentiation by displacement of the repressive complexes and chromatin marks. While genes de-repressed during differentiation are lineage specific, non lineage specific genes specifically remain occupied and repressed by PcG proteins. This mechanism reveals a dynamic role for PcG complexes and their chromatin modifications during differentiation [1, 38, 39].

Lee and colleagues found that genes bound by the important transcription factors OCT4, SOX2, and NANOG, required for the propagation of undifferentiated embryonic stem cells (ESCs) in culture were almost all additionally occupied by PRC2. This shows a link between repression of developmental regulators and stem cell pluripotency [38]. The pluripotency genes Oct4 and Nanog were associated with low levels of H3K27me3 in ESCs as well as in differentiated neuronal progenitor (NP) cells, suggesting silencing by different mechanisms. [39]. A majority of identified target genes in fibroblasts had homologues previously identified as PcG targets in *Drosophila* [1].

10-20% of PcG target cells are actively transcribed in embryonic stem cells, and a large proportion (about 2%) of PcG-bound genes are also occupied by Polymerase II [40]. Genes occupied by PRC1, PRC2 and Polymerase II, are called bivalent domains. This chromatin signature renders the respective developmental genes poised for activation, so that induction of transcription upon differentiation stimuli can occur extremely rapidly [21]. Bivalent domains are not only found in ESCs, but also in other stem cells, such as mesenchymal stem cells and hematopoietic stem and progenitor cells [21].

The role of EZH2 in stem cell maintenance and differentiation

Embryonic stem cells (ESCs) are pluripotent cells and have the potential to differentiate into all cell types of an embryo except the trophoectoderm [21]. PcG proteins are involved in the repression of early differentiation marker genes to maintain the pluripotency of ESCs in the embryonic stage [14]. EZH2 is highly expressed in ESCs and required for early mouse development [15]. EZH2 expression is associated with undifferentiated, proliferating cells. During differentiation and development EZH2 transcript levels are downregulated, while EZH1 levels increase [15]. EZH2 has also been shown to be involved in the maintenance of adult stem cells (ASCs) [41] as well as in the differentiation of ESCs or ASCs into several cell lineages [14]. However stem cell maintenance not only requires a complete PRC2, but also its downstream partner PRC1 [21].

A stem cell link to cancer

The existence of cancer stem cells was first clearly demonstrated in leukemia. Many types of cancer cells can be organized into hierarchies, leading from malignant cancer stem cells, which have high proliferative potential, to differentiated cancer cells with a limited differentiation potential [42]. The cancer stem cell compartment shares with normal stem cells an unlimited potential for self-renewal and the ability to differentiate in many cell types [43]. Cancer stem cells are highly tumorigenic and can be as rare as 0.1% of the total tumor mass. They are believed to be the source of tumor progression, metastasis, and recurrence and are resistant to conventional therapy [43]. In some cases cancer stem cells may arise from mutated normal stem cells and in other cases from restricted progenitors or differentiated cells which acquire stem cell characteristics such as self-renewal potential. [42]. These cells also express various stem cell-specific genes, including Nanog, Oct3-4 and c-Myc in whose expression Polycomb repressive complexes play important roles [43].

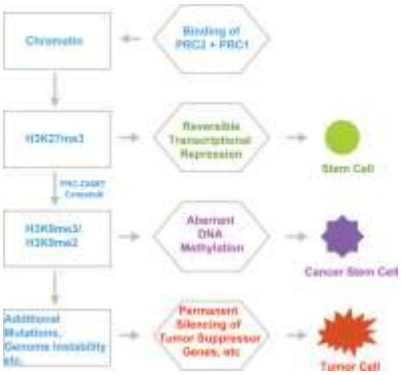

Figure 4. Adapted from Rajasekhar et al. 2007. "*Schematic model of epigenetic changes in the onset of cancer.* *Graded progression of epigenetic marks from reversible gene repression in stem cells (including embryonic stem cells) via transiently aberrant promoter DNA hypermethylation in cancer stem/precursor cells (embryonal carcinoma cells) to the "locked-in state" of gene silencing in cancers (e.g., tumor cells). Abbreviations: DNMT, DNA methyltransferase; PRC, Polycomb repressive complex*" **[6]**.

The role of EZH2 in cancer

EZH2 has been associated with cell proliferation, cancer progression and unfavorable clinical outcome in many tumor types such as prostate cancer [44-46], breast cancer [44], melanoma [44], endrometrial carcinoma [44], lung cancer [47], bladder cancer [47], colorectal cancer [47, 48], nasopharyngeal carcinoma [27], and many more.

EZH2 in prostate cancer

For a current review on general prostate cancer epigenetics see [4]. Prostate cancer is one of the leading causes for cancer related death in American men second only to lung cancer [45]. Prostate cancers are usually treated by hormone ablation therapy to which the majority of tumors initially respond well. However, disease often recurs in the form of hormone refractory prostate cancer which is more aggressive and refractory to cure [49].

EZH2 was reported to be significantly upregulated in metastatic prostate cancer as compared to clinically localized prostate cancer on mRNA as well as on protein level [45]. Varambally and colleagues reported a trend towards increased expression of EZH2 protein as prostate neoplasia progresses and propose a correlation of EZH2 expression

levels with prostate cancer aggressiveness and clinical outcome [45]. EZH2 expression in prostate cancer was reported to be an independent predictive marker of cancer recurrence [44, 46].

By combining chromatin-immunoprecipitation (ChIP) with promoter assays, Yu and colleagues (2007) mapped genomic sites occupied by PRC2 in late-stage, aggressive prostate cancer tissues and identified genes directly repressed by PRC2 [46]. By selection of a common set of H3K27me3-occupied genes of two metastatic prostate tumors, this group was able to identify an 87 gene Polycomb repression signature in metastatic prostate cancer. A refined 14-gene signature enabled them to predict patient survival with high significance in two prostate and six breast cancer data sets a finding consistent with EZH2 up-regulation in aggressive tumors [46].

Gene Symbol	Gene Name
CTSG	Cathepsin G
CXCL12	Chemokine (C-X-C motif) ligand 12 (stromal cell-derived factor 1)
DARC	Duffy blood group, chemokine receptor
EPHB6	EPH receptor B6
FST	Follistatin
ITGB2	Integrin, beta 2 (complement component 3 receptor 3 and 4 subunit)
KRT17	Keratin 17
NCKAP1L	NCK-associated protein 1-like
PRKG1	Protein kinase, cGMP-dependent, type I
PTGER3	Prostaglandin E receptor 3 (subtype EP3)
RLN1	Relaxin 1
SNCA	Synuclein, alpha (non A4 component of amyloid precursor)
SOCS2	Suppressor of cytokine signaling 2
WNT2	Wingless-type MMTV integration site family member 2

Figure 5. The refined 14 "Polycomb Repression Signature" genes proposed by Yu and colleagues (in supplementary data available at: http://cancerres.aacrjournals.org/content/suppl/2007/11/12/67.22.10657.DC1/CAN_11-15-07_Yu.pdf (11.01.12))**.** The down-regulated expression of these genes is associated with poor clinical outcome [46].

EZH2 in breast cancer

Breast cancer is the second most common cause of death in women in the Western world [50]. EZH2 is highly overexpressed in breast cancer metastases [51]. Introduction of EZH2 into normal immortalized breast epithelial cells promotes anchorage-independent growth and cell invasion which is dependent on a functional SET domain and histone deacetylases [51]. EZH2 is regulated by cell growth in normal cells and it accumulates at the G1/S transition. This regulation nevertheless is lost in cancer cells [50]. Gonzalez et al propose that EZH2 knockdown in breast cancer cells leads to

reduced proliferation due to upregulation of the tumor suppressor protein BRCA1, which is involved in DNA repair and G2/M arrest [50]. EZH2 is an independent prognostic predictor of breast cancer recurrence and death and provides prognostic information above and beyond other known clinical and pathological markers [51].

Lee and colleagues report a role of EZH2 in upregulation of NF-κB target gene expression in Estrogen receptor negative (ER-negative) basal-like breast cancer cells in a previously undiscovered complex with RelA and RelB. The methyltransferase activity is not required for this function. Strikingly, in ER-positive luminal-like breast cancer cells EZH2 has exactly the opposite effect in the context of PRC2 and represses NF-κB target gene expression by directing repressive histone methylation to their promoters and by interacting with ER [52].

EZH2 was reported as a valuable independent prognostic marker also in colorectal cancer [47]. Knockdown of EZH2 by siRNA was reported to reduce proliferation in two bladder cancer cell lines, two lung cancer cell lines and one colorectal cancer cell line [47]. In another recent study the knockdown of EZH2 in 3 colon cancer cell lines reduced cell proliferation and changed the expression level of several genes involved in the control of cellular development, growth, cellular movement, and signaling. [48]. Cell cycle analysis of various tumor cells showed accumulation of cells in the G1 phase [47, 48].

Heterozygous EZH2 point mutation in B-cell lymphomas

Sequencing of B-cell lymphoma cells led to the identification of a heterozygous somatic mutation in the SET domain of EZH2 at tyrosine 641 in follicular lymphoma and the germinal-center B-cell like (GCB) subtype of diffuse large B-cell lymphoma. This mutation was reported to render the protein unable to perform trimethylation in an in vitro methylation assay of an H3K27 peptide [53]. The mutation affecting Tyr 641 is one of the most frequent mutations observed in GCB malignancies after t(14;18)(q32;q21) translocation [53]. Sneeringer and colleagues made the exciting discovery that the

mutant enzymes (Y641F, Y641H, Y641N, and Y641S) are defective in catalyzing the initial step of H3K27 monomethylation, but more efficient than the wild type (WT) enzyme in catalyzing the subsequent steps leading from monomethyl to di- and tri-methyl H3K27 [54] (Figure 6).

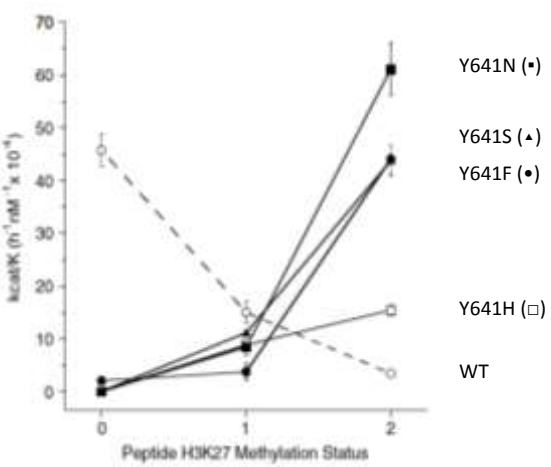

Figure 6. Adapted from Sneeringer et al. 2010. "*PRC2 complexes containing mutant EZH2 preferentially catalyze di- and trimethylation of histone H3K27.* *Catalytic efficiency (kcat/K1/2) decreases with increasing K27 methylation states for wild-type (○) but increases for Y641F (•), Y641H (□), Y641N (•), and Y641S (▲) mutants of EZH2. The lines drawn to connect the data points are not intended to imply any mathematical relationship; rather, they are intended merely to serve as a visual aid to guide the eye of the reader*" [54].

The H3K27 demethylase UTX was found to be somatically mutated in many cancer types, mainly multiple myeloma, esophageal squamous cell carcinomas, and renal cell carcinomas. Upon UTX re-expression in UTX null cells, cell doubling time was significantly increased. Furthermore, changes in gene expression were observed with an enrichment for H3K27me3 marked genes [12]. Loss of UTX activity would be enzymatically equivalent to a gain of function for EZH2. In each situation the steady state level of trimethylated H3K27 would be increased in cancer cells [54].

In conclusion, increased trimethylation of target genes in various types of cancer can occur by several mechanisms (Figure 7).

Mechanisms of H3K27 hypertrimethylation

- EZH2 can be mutated like it is the case in many B-cell lymphomas and thereby have increased activity for di- and tri-methylation of H3K27 [53, 54].
- EZH2 can be overexpressed as it is the case in a broad panel of cancer types from prostate [44-46], and breast cancer [44], melanoma [44], endrometrial carcinoma [44], lung cancer [47], bladder cancer [47], colorectal cancer [47, 48], nasopharyngeal carcinoma [27] etc.
- The EZH2 gene can be amplified as it is frequently the case in melanomas [55].
- Mutation or deletion of the histone H3K27 demethylase UTX leads to an overall increase of H3K27 methylation [12].
- Deregulation of factors modulating the activity of PRC2 can increase H3K27. Critical examples are overexpression of PHF19 [54], downregulation of miR-101 in prostate cancer [30-32] and pancreas carcinoma [32, 33] and a deregulation of the pRB-E2F pathway [28].

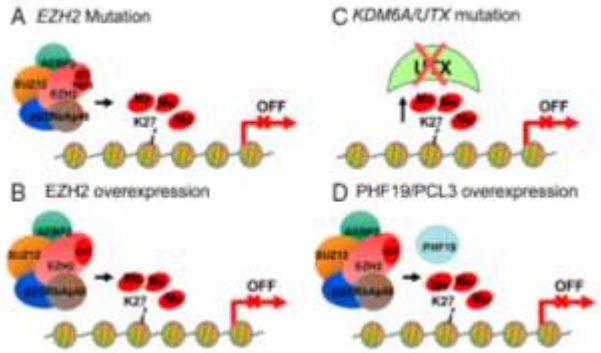

Figure 7. Adapted from Sneeringer et al. 2010. ***"Proposed mechanisms leading to aberrantly high levels of trimethylation on histone H3K27 in cancer include*** *(A) mutation of Y641 in EZH2 resulting in a change in substrate preference from the nonmethylated to the mono- and dimethylated histone H3K27, (B) overexpression of EZH2, (C) mutations in UTX that inactivate enzyme function, causing a decrease in demethylation of H3K27me3, and (D) overexpression of the PRC2 complex subunit HF19/PCL3 that leads to increases in recruitment of the PRC2 complex to specific genes and an increase in histone H3K27 trimethylation. In all four models the alteration leads to aberrant histone H3K27 trimethylation in the proximal promoter regions of genes resulting in transcriptional repression of key genes in cancer*" [54].

THESIS RATIONALE

To determine whether EZH2 is a potential target for cancer therapy in multiple cancer types, we evaluated the effect of EZH2 knockdown in a panel of different human cancer

cell lines. EZH2 has been reported to increase cancer cell proliferation and to serve as an independent prognostic marker for patient outcome in many studies [44, 45, 47]. However, we wanted to compare the effect of EZH2 knockdown in different cell lines with various alterations of EZH2. For this reason, the following cell lines were chosen to perform this study: C32 (EZH2 gene amplification), EVSA-T (EZH2 overexpression), MiaPaCa-2 (UTX deletion), Karpas-422 and SU-DHL-6 (EZH2 point mutation). We also used three prostate cancer cell lines, two of which were androgen insensitive (PC3, DU-145) and one was androgen sensitive LNCaP.FGC. These experiments should help in defining the patient population which could be potentially responsive to an EZH2 inhibitor. We performed stable EZH2 knockdown by short hairpin RNA (shRNA), which was introduced into cells via lentiviral transfection and stably integrates into the genome of the host cells. To obtain cell populations with homogenous EZH2 knockdown, we selected cells which had integrated the lentivirus into their genome by the antibiotic puromycin. The EZH2 knockdown cells were seeded at low cell densities and followed-up by a confluence based and a metabolism based cell proliferation assay for a period of 14 days. EZH2 protein knockdown and global H3K27me1, H3K27me2, and H3k27me3 levels were determined by Western blot. In parallel, we assessed EZH2 and EZH1 mRNA levels by real time quantitative PCR (RT q-PCR).

We chose two cell lines for a soft agar colony formation assay which measures the ability of cells for anchorage independent growth [51]. To confirm an effect of EZH2 knockdown on target gene expression, we chose 10 published EZH2 target genes and performed RT q-PCR in three selected cell lines. We chose three target genes of the 14-target gene signature in cancer proposed by Yu and colleagues [46] and seven others based on various publications with interesting aspects of cancer.

ABBREVIATIONS

ASC	Adult stem cell

AB	Antibody
cDNA	complementary DNA synthesized from cellular mRNA
EED	Ectoderm endoderm development
ER	Estrogen receptor
ESC	Embryonic stem cell
EZH1	Enhancer of zeste homolog 1
EZH2	Enhancer of zeste homolog 2
EDTA	Ethylenediaminetetraacetic acid
FBS	Fetal Bovine Serum
FL	Follicular lymphoma
CSI	Genetix CloneSelect™ Imager
gDNA	genomic DNA
GCB	Germinal-center B-cell like lymphoma
H3K27	Lysin 27 on Histone H3
H3K27me1	Monomethylated H3K27
H3K27me2	Dimethylated H3K27
H3K27me3	Trimethylated H3K27
HKDM	Histone lysine demethylase
HMTase	Histone methyl transferase
HRP	Horse raddish peroxidase
IgG	Immunglobulin G
miRNA	micro RNA
mA	milliampere
MEM	Minimal Essential Medium
NCBI	National Center for Biotechnology Information
NTC	Non targeting control
RefSeq	NCBI Reference Sequence
NEAA	Non essential amino acids
PAA	Polyacrylamide
PAGE	Polyacrylamide Gelelectrophoresis
PBS	Phosphate buffered saline
PcG	Polycomb group genes
PRC1	Polycomb repressive complex 1
PRC2	Polycomb repressive complex 2
RIPA Buffer	Radioimmunoprecipitation assay buffer
rcf	relative centrifugal force
RT q-PCR	Reverse Transcription quantitative Polymerase Chain Reaction
shRNA	short hairpin RNA
siRNA	short interfering RNA
SDS	Sodium dodecyl sulfate
SUZ12	Suppressor of zeste 12
TRX	Thioredoxin
TrxG	Thritorax group Proteins
TXNIP	Thioredoxin interacting protein

WT	Wild type

MATERIALS AND METHODS

General Cell Culture Work

All cell culture work was carried out under sterile conditions in a lamina air flow. Cells were cultured in media without antibiotics.

Cell Lines

Cell Line	Organ	ATCC/DSMZ number	Cell Batch ID	Growth type	Medium	Split Ratio
EVSA-T	breast	ACC 433	26929	adherent	MEM, 10% FBS, Glutamax, 25mM HEPES	1:6
SU-DHL-6	lymphatic system	ACC 572	27062	suspension	RPMI1640 + GlutaMAXTM-I, 20% FBS	1:25
MIA PaCa-2	pancreas	CRL-1420	26909	adherent	DMEM, 10% FBS, NEAA, NaPyruvate	1:8
Karpas-422	peripheral blood	ACC 32	27157	suspension	RPMI1640 + GlutaMAXTM-I, 20% FBS	1:4
OCI-LY-19	peripheral blood	ACC 528	27063	suspension	MEM, 20% FBS, Glutamax	1:10
DU 145	prostate	HTB-81, ACC 261	26920	adherent	F-12 + GlutaMAXTM-I (Ham), 10% FBS	1:3
LNCaP.FGC	prostate	CRL-1740	26836	adherent	IMDM + GlutaMAXTM-I, 10% FBS	1:4
C32	skin	CRL-1585	26921	adherent	EMEM, 10% FBS, Glutamax	1:3
PC-3	prostate	CRL-1435	27525	adherent	F-12 + GlutaMAXTM-I (Ham), 10% FBS	1:4

Table 1. List of cell lines

Passaging of cells

Adherent cells:

The cell culture medium was aspirated, cells were rinsed with warm PBS and were covered with Trypsin/EDTA according to the size of the culture flask (25cm^2: 1ml, 75cm^2:

2ml, 175cm^2: 3ml). The cells were detached by carefully tapping the flask and the trypsinization reaction was stopped by addition of cell culture medium containing fetal bovine serum (FBS). The cells were thoroughly resuspended and passaged according to split ratios (Table 1.).

Suspension cells

Suspension cells were diluted in fresh medium according to split ratios.

The cells were incubated at 37°C and 5% CO_2.

Determination of cell number and viability

Cell counting and the determination of cell viability was carried out by the Beckman coulter Vi-CELL XR Cell Viability Analyzer according to the manufacturer's instructions.

The Vi-CELL is a cell counting machine working on the principle of a cell counting chamber and is able to also count clumped cells. It automatically aspirates samples, mixing them with trypane blue, counting cells in a flow cell by using a camera, averaging 50 individual pictures, and cleaning the system before the uptake of the subsequent sample. The uptake of trypane blue into cells indicates a permeabilized membrane of dead cells thereby allowing assessment of cell viability.

Freezing of cells

Adherent Cells were detached by trypsinization and the reaction was stopped with cell culture medium containing FBS before transferring the cells into a 50ml falcon. Suspension cells were directly transferred into appropriately sized falcon tubes. Cell number and viability were assessed by the Vi-CELL and the tubes were centrifuged for 5 minutes at 201rcf at room temperature (RT). The supernatant was discarded and the cells were resuspended in Cryostore solution. 1ml aliquots of cell suspension were transferred into cryotubes, which were placed in a "Mr. Frosty" Cryo 1°C Freezing Container and frozen at -80°C. The "Mr. Frosty" container is filled with Isopropanol which cools the cells 1°C per minute.

Thawing of cells

The cells were thawed at 37°C and immediately transferred to appropriately sized cell culture flasks filled with warmed cell culture medium. A dilution of Cryostore of at least 1:10 is necessary to not harm the freshly thawed cells. The following day a media change was carried out. The cells were split at least three times before using them in experiments to ensure total recovery of the cells after thawing.

Cell Culture Media	Company	Cat. No.
DMEM Dulbeccos's Modified Eagle Medium with 4.5g/L Glucose, with L-Glutamine	Lonza	BE12-604F
EMEM Minimum essential Medium Eagle with NEAA and NaPyruate, without L-Glutamine	Lonza	BE-12662F
F-12 + GlutaMAX™-I Nutrient Mixture (Ham) 1X	Invitrogen	31765
IMDM + GlutaMAX™-I Iscove's Modified Dulbecco's Medium 1X with 25mM HEPES	Invitrogen	31980
McCoy's 5A + GlutaMAX™-I without Serum	Invitrogen	36600
MEM Minimal Essential Medium 1X with Earle's, without L-Glutamine	Invitrogen	21090
RPMI 1640+GlutaMAX™-I 1X	Invitrogen	61870

Table 2. Cell Culture Media

Chemicals for Cell Culture	Company	Cat. No.
1M HEPES pH 7,3	Affymetrix/USB	16924
Cryostore Solution	BioLife Solutions	210102
DPBS 1X	Invitrogen	14190
Fetal Bovine Serum (FBS)	JRH Biosciences	12103-1000M
Glutamax 100X	Invitrogen	35050-038
MEM Non Essential Amino Acids (NEAA) 100X	Invitrogen	11140
Sodium Pyruvate	Invitrogen	11360
Trypsin EDTA in PBS	Invitrogen	043-90317FU
Ethanol	Merck	1.00971.2500

Table 3. Chemicals for Cell Culture

shRNA Experiments

Cells were transduced with lentiviruses carrying short hairpin RNAs (shRNAs). Upon integration of the reverse transcribed lentiviral genome into the host genome they lead

to stable downregulation of a defined mRNA product by the small interfering (siRNA) machinery of mammalian cells over numerous cell generations.

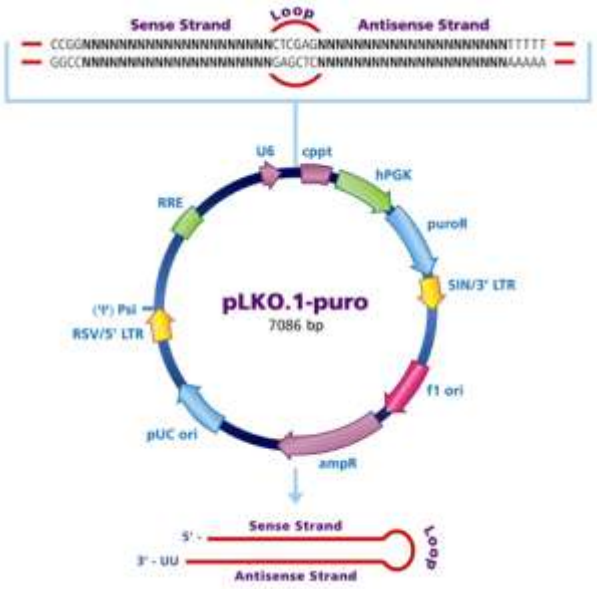

Figure 8. Illustration of MISSION® shRNA Lentiviral Transduction Particles ***(http://www.sigmaaldrich.com/catalog/ProductDetail.do?lang=de&N4=SHC002H|SIGMA&N5=SEARCH_CONCAT_PNO|BRAND_KEY&F=SPEC; 06.12.11)*.**

Experiment Summary

Cells were transduced with lentivirus in 12-well culture plates, the medium was changed the following day and again one day later, cells, which had integrated the lentivirus into their genome, were selected by adding puromycin to the cell culture medium. Five days after transduction the cells were seeded in 96-well plates for further experiments such as cell proliferation assays and reverse transcription quantitative PCR (RT q-PCR). Additionally, the knockdown of EZH2 as well as global changes in histone H3 methylation status were determined by Western blot of whole cell lysates prepared 3 to 14 days after seeding in 12-well plates (Figure 9).

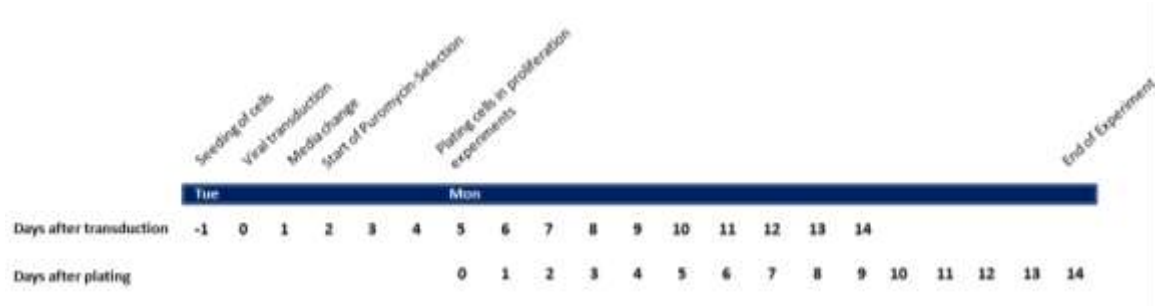

Figure 9. Lentiviral protein knockdown: experiment overview

Materials	Company	Cat. No.
MISSION® Non-Target shRNA Control Transduction Particles	Sigma	SHC002H
MISSION® shRNA Lentiviral Transduction Particles	Sigma	NM_004456
Puromycin dihydrochloride, 10mg/ml in H2O	Sigma	P9620

Table 4. Materials for shRNA transduction

Sigma MISSION anti EZH2 Lentiviruses NM_004456

TRC Number	Clone ID	Targeted region	Sequence
TRCN0000010**475**	NM_004456.x-2450s1c1	3' UTR	CCGGAAACAGCTGCCTTAGCTTCACTCGAGTGAAGCTAAGGCAGCTGTTTCTTTTTG
TRCN0000018**365**	NM_004456.x-2278s1c1	CDS	CCGGTATGATGGTTAACGGTGATCACTCGAGTGATCACCGTTAACCATCATATTTTTG
TRCN0000040**077**	NM_004456.3-950s1c1	CDS	CCGGCCCAACATAGATGGACCAAATCTCGAGATTTGGTCCATCTATGTTGGGTTTTTG
TRCN0000040**074**	NM_004456.3-1544s1c1	CDS	CCGGGCTAGGTTAATTGGGACCAAACTCGAGTTTGGTCCCAATTAACCTAGCTTTTTG
TRCN0000040**075**	NM_004456.3-440s1c1	CDS	CCGGCCAACACAAGTCATCCCATTACTCGAGTAATGGGATGACTTGTGTTGGTTTTTG

Table 5. Sigma MISSION anti EZH2 Lentiviruses

Determination of optimal puromycin concentrations

Cells were seeded in a 96-well plate and treated with different concentrations of puromycin (0, 0.5, 1, 2, 4, 8µg/ml) in triplicates 1 day after plating. 3 days later cell

metabolism was measured by an Alamar Blue assay and the minimum concentration of puromycin to completely kill all non transduced cells was determined.

Lentiviral transduction

Adherent Cells

Cells were seeded at 200 000 cells/well in 12-well culture plates in media appropriate for the corresponding cell lines. The following day the cells were transduced with lentivirus by adding lentiviral particles at a multiplicity of infection (MOI) of 4 to 6. The MOI describes the number of virions statistically infecting a single cell. The plates were gently shaken to mix the virions with the cell culture medium and incubated over night at 37°C, 5% CO_2. To remove leftover virions from the culture medium, the cells were carefully washed with warm PBS and supplied with fresh culture medium. To select for cells that have lentivirus incorporated into their genomes, selection with puromycin was started the following day. Puromycin is an antibiotic derived from the bacterium *Streptomyces alboniger* that inhibits protein synthesis by causing premature chain termination [56, 57]. The shRNA lentiviruses carry the resistance gene puromycin N-acetyl-transferase (PAC) [58] and allow cell survival upon successful incorporation into the genome of virus treated cells. The cell culture medium was aspirated and replaced by selection medium containing puromycin in a concentration suitable for the respective cell line. Optimal puromycin concentrations determined in kill-curve experiments were usually in a range of 2 up to 4µg/ml puromycin. Faster growing cells (e.g. EVSA-T or MiaPaCa-2) that had already reached a confluence of above 80% at the day of selection were detached with trypsin and transferred to 6-well plates in 2ml total selection medium. Incubation with selection medium was carried out for 72h. After selection the cells were detached with trypsin, viability and cell number were assessed by the Vi-CELL and they were seeded for experiments at low cell densities in 96- and 12-well plates (96-well plates: triplicates of 200, 800 and 1600cells/well; 12-well plates: 1000, 4000, 8000cells/well, one well per condition for production of whole cell lysates). Transduced cells were at all times kept in medium containing puromycin, usually in concentrations used for the initial selection. The medium containing puromycin was changed twice a week.

Suspension cells

Suspension cells were seeded at 200 000 cells/well in 12-well plates and transduced with lentivirus the same day at an MOI of 4 to 6. The plates were gently shaken to mix the virions with the cell culture medium. To increase the efficacy of transduction the plates were sealed with parafilm and centrifuged for 5min at 201rcf before incubation at 37°C for two days. This step is sedimenting cells as well as viral particles to the bottom of the plate in order to increase the probability of virions infecting the cells [59]. For puromycin selection cells were transferred to 1.5ml Eppendorf-tubes and spinned for 5min at 201rcf. The supernatants were carefully removed, cells were resuspended in 1.5ml selection-medium and transferred into a new 12-well plate.

To assure adequate selection, the viability and cell number of non-transduced cells previous and after treatment with puromycin was determined in the respective experiments.

After 3 days of selection the cells were counted and seeded in 96-well plates for experiments. To measure cell proliferation, a metabolic assay was performed 3 and 7 days after plating of the cells.

Cell Proliferation Assays

Measurement of confluence with the Genetix CloneSelect™ Imager (CSI)

The CloneSelect™ Imager is an instrument that optically measures the confluence of cells in microplates. The measurements are carried out under sterile conditions (the lids of the microplates remain closed), and in a non invasive manner, allowing to follow the growth of cells in a single well over a prolonged period of time. Microplates of different manufacturers and of various well formats (6-well, 12-well, 24-well, 96-well) can be measured.

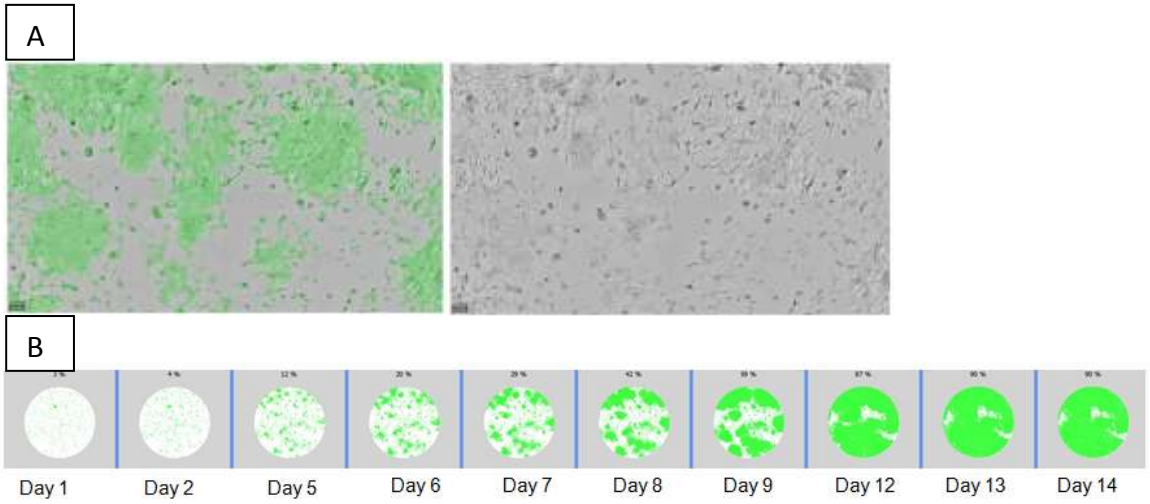

Figure 10. Daily CSI proliferation measurement based on cell confluence. (A) The Clone Select Imager is a microscopic device that can automatically determine areas of cell growth. **Right panel**: A microscopic picture of the cells is taken (LNCaP.FGC); **left panel**: cells are detected and a confluence value for the whole well is calculated. **(B)** The confluence of a single plate can be measured on a daily basis without contamination of the cells or long periods of time at room temperature.

The confluence of cells seeded in triplicates in 96-well plates was measured on a daily basis by the clone select imager up to 14 days after seeding. The plate was loaded onto the plate carrier and wells to be measured were selected. Before measurement focus, cell detection method and brightness were adjusted according to cell line and well format.

Typical settings for a BD Falcon 96-well plate (Cat.No. #35 3072) were:

- Focus: 951
- Brightness: 75%
- Cell detection method: 1 or 2 (Table 6)

Cell line	Cell detection method
C32	2
DU-145	2
EVSA-T	2
LNCap.FGC	1
MIA PaCa-2	2
PC3	2

Table 6. Cell detection methods used in the CSI cell proliferation assay. The selected cell detection method uses certain algorithms to detect adherent cells and is chosen according to cell shape and growth type.

The results were analyzed in Microsoft Office Excel. Mean values as well as standard deviation were calculated for the triplicates.

2 D Alamar Blue assays measuring metabolism

Assay Principle:

Metabolically active cells reduce the non-fluorescent chemical resazurin to the red-fluorescent molecule resofurin which can be detected by fluorimetric measurement. The reaction is proportional to the number of viable cells in a well and the reaction is linear over a wide range of cells and time.

Alamar Blue assays are a valuable tool to estimate the proportion of living cells especially in suspension cells where measurements of confluence are impossible.

The assay was performed according to the manufacturer's instructions. 20µl of Alamar Blue reagent were added to wells filled with 200µl of cell culture medium and incubated at 37°C, 5% CO_2. After 3 up to 24 h, depending on the cell line, cell number and rate of metabolism, the fluorescence of the wells was measured in a Gemini XPS Fluorescence Microplate Reader (Molecular Devices) at an extinction wavelength of 530 and an emission wavelength of 592nm.

Mean values and standard deviations of the triplicates were calculated in Microsoft Office Excel.

Material	Company	Cat. No.
AlamarBlue	AbD Serotec	BUF012B

Table 7. Materials for the metabolic Alamar Blue cell proliferation assay

Soft agar colony formation assay

In this assay cells were embedded into a non floating 0.3% agarose-medium mixture. Proliferating cells do not have a flat surface for growth as under normal culture conditions, but have to expand three dimensionally facing challenges such as contact inhibition and reduced availability of nutrients. The ability to grow in 3D allows evaluating the metastatic potential of cells [51].

A 96-well plate was coated with a 1.2% agarose bottom layer by diluting molten 3% agarose in warmed cell culture medium at 37°C in a heating block. 110µl of bottom layer were pipetted into the wells and allowed to harden at room temperature. Cells were trypsinized, counted and diluted at 14 300 cells/ml in warm selection medium containing 0.3% agarose again in a heating block. 70µl of cell suspension (corresponding to 1000 cells/well) were added on top of the bottom layer. After hardening of the gel, 20µl of cell culture medium was added to the wells to prevent drying out of the agarose gel. The plate was incubated at 37°C, 5% CO_2. To increase the humidity and prevent drying of the agarose, the plate was incubated in a plastic container supplied with a vessel containing distilled water. The forming cultures were inspected microscopically on a daily basis. Upon formation of round shaped three-dimensional cultures the wells were incubated with 20µl per well Alamar Blue reagent to measure metabolism for 3 up to 24 hours depending on cell number and metabolism.

Materials	Company	Cat. No.
Agarose 4%	Invitrogen	18300
Growth medium dependent on cell line		

Table 8. Materials for the soft agar colony formation assay

Determination of Protein knockdown and Biomarker status

Preparation of whole cell lysates

Cells were incubated in 12-well plates at low cell densities (usually 5 days after viral transduction) and lysed 8-14 days after plating to determine protein knockdown and the methylation status of histone H3K27.

Adherent cells:

The cell culture medium was aspirated, the culture dishes were placed on ice and cells were washed with ice cold 1xPBS. Depending on cell number and confluence the cells were lysed with 80-150µl RIPA Buffer (50mM TRIS-HCL pH 7.4, 150mM NaCl, 0,25% Sodium deoxycholate, 1% Triton X-100, 1mM EDTA, 0,1% SDS, Proteaseinhibitor-cocktail

Complete). Cells in lysis buffer were scraped from the plate and transferred to 1.5ml Eppendorf tubes. They were incubated by rotation at 4°C for 15 minutes, sonicated four times in a 4°C water bath at an amplitude of 35 and frozen at -80°C. The lysates were at all times kept on ice.

Suspension cells:

Cells were transferred to 1.5ml Eppendorf tubes and centrifuged for 5 minutes at 201rcf, room temperature. The supernatants were discarded, the cells were washed by resuspension in 1ml 1xPBS and again centrifuged. After removal of the supernatant the cells were resuspended in 100-200µl RIPA buffer. Cells in lysis buffer were incubated by rotation at 4°C for 15 minutes, sonicated four times in a 4°C waterbath at an amplitude of 35 and stored at -80°C.

Materials	Company	Cat.No.
1M TRIS-HCL pH 7,4	Lonza AccuGene	51237
5M NaCl	Lonza AccuGene	51202
Triton X-100 solution	Fluka	93443
20% Sodium dodecyl sulfate Solution (SDS)	USB	75832
Proteaseinhibitorcocktail Complete Mini EDTA free (PI)	Roche	11873580001
Sodium deoxycholate	Merck	6504
Ethylenediaminetetraacetic acid (EDTA)	Fluka	101042100

Table 9. Materials for whole cell lysates

Western Blot

Determination of Protein concentration

The protein concentration of the whole cell lysates was determined by the Bio Rad Protein Assay utilizing the Bradford method. The Bradford reagent was diluted 1:5 in ddH_2O and 2-4µl of thoroughly vortexed lysates were mixed with 1ml Bradford solution in plastic cuvettes. The absorbance at 595nm was measured in an *Eppendorf BioPhotometer plus* and the protein concentrations were calculated according to a BSA standard curve.

Materials	Company	Cat.No.
Bio-Rad Protein Assay Dye Reagent Concentrate	Bio-Rad	500-0006
Bovine Serum Albumin (BSA)	Serva	11945

Table 10. Materials for Bradford Protein concentration determination

SDS-Polyacrylamid Gelelectrophoresis (SDS-PAGE)

The lysates were diluted with ddH_2O and 4x Loading buffer to 3-5µg total protein in 20µl. The samples were denatured for 5 minutes at 95°C, spinned down shortly and loaded onto 26-well TGX Precast Gels (4-12% Bis Tris). Protein separation was performed for 60 minutes at 150 Volt in XT-MES running buffer.

Materials	Company	Cat.No.
Roti-Load 4x Loading Buffer	Roth	K929.1
Criterion XT Bis-Tris Gel, 4–12%, 26-well, 15 µl, 13.3 x 8.7 cm (W x L)	Bio-Rad	345-0125
Precision Plus Protein Dual Color Standards	Bio-Rad	161-0374
XT MES Running Buffer	Bio-Rad	161-0789

Table 11. Materials for SDS Page

Western Blot (Semi-dry)

After protein separation by SDS-PAGE the protein bands were blotted onto a membrane and stained with specific primary and secondary antibodies.

The gel was placed onto a stack of a thick and a thin filter papers covered by a Nitrocellulose blotting membrane. Onto the gel another thin and thick filter paper was placed and air bubbles were removed by using a roller. All the components were soaked in Towbin Buffer (20% Methanol, 1x Tris/Glycine in H_2O) before use.

Band transfer was carried out at 170mA per gel for 60 minutes.

In order to inhibit unspecific binding of antibodies to the membrane, the latter was blocked for at least 1h at room temperature shaking in Roti Block blocking solution. The blot was cut into appropriate fragments, labeled with a pencil and incubated with primary antibody solution, diluted in blocking buffer, at 4°C over night. The following

day the membrane was shortly rinsed with ddH_2O and washed 3 times 10 minutes with PBST [1x PBS, 0.05% Tween 20]. It was then incubated with near infrared fluorescently labeled secondary antibody diluted 1:5000 in 10% Casein in PBST [0.05% Tween 20] for 1-2h at RT in the dark. After washing 3 times 10 minutes with PBST the membrane was placed in PBS and the signals of the secondary antibodies were detected by a *LI-COR Odyssey Infrared Imager*.

Materials	Company	Cat.No.
Nitrocellulose/Filter Paper Sandwiches	Bio-Rad	162-0235
Extra Thick Blot Paper, for Criterion gels, 8 x 13.5 cm	Bio-Rad	1703967
10x Tris/Glycine	Bio-Rad	161-0771
Methanol	Merck	1.06009.2500
Roti-Block 10x Blocking Buffer	Roth	A151.2
10% Tween 20	Bio-Rad	161-0781
10x Dulbecco's Phosphate Buffered Saline (DPBS)	Gibco	792643

Table 12. Materials for Western Blot

Primary Antibodies	Company	Cat. No.	Species	Dilution	Size
Anti-monomethyl H3K27	active motif	39377	rabbit	1:1000	17kDa
Anti-dimethyl H3K27	Cell signaling	9755L	rabbit	1:2000	17kDa
Anti-trimethyl H3K27	Millipore	ABE44	rabbit	1:30 000	17kDa
AR (N-20)	Santa Cruz Biotechnology	sc-816	rabbit	1:500	110kDa
Beta Actin	Abcam	ab8226	mouse	1:5000	42kDa
Cleaved caspase 3 (Asp175)	Cell signaling	9661L	rabbit	1:1000	17kDa
EZH2	BD Transduction Lab	612667	mouse	1:1000	91kDa
GAPDH	Abcam	ab8245	mouse	1:10 000	40kDa
Histone H3	Cell signaling	3638	mouse	1:2000	17kDa
PARP	Cell signaling	9542L	rabbit	1:1000	116kDa (uncleaved) 89kDa (cleaved)

UTX	Bethyl	A302-374A	rabbit	1:2000	160kDa
EZH1	Abcam	ab13665	rabbit	1:500	95kDa
EZH1	Sigma Aldrich	SAB2500373	goat	1:500	85kDa
EZH1	Abcam	ab64850	rabbit	1:1000	85kDa
EZH1	Thermo Scientific	PA1-31771	goat	1:500	85kDa to 95kDa
Secondary Antibodies					
Alexa Fluor 680 goat anti-mouse IgG (H+L)	Invitrogen	A21058			
Alexa Fluor 680 goat anti-rabbit IgG (H+L)	Invitrogen	A21109			

Table 13. List of Antibodies used for Western Blot

Quantification of Western Blot Bands

Western blot bands were quantified using the GE Healthcare Image Quant Software. Background values were defined for every lane and the average intensity levels were subtracted from the respective bands of specific antibody. EZH2 levels were normalized to GAPDH or β-actin and H3K27me1, H3K27me2 and H3K27me3 levels were normalized to total H3. Values obtained for EZH2 knockdown samples were calculated in percent of the respective controls.

siRNA experiments

Cells were reverse transfected with siRNA in 6-well plates and 5 days later again forward transfected to ensure consistent protein knockdown. From the first day of plating cell proliferation was measured daily by the Clone Select Imager.

Reverse transfection:

4µl of Lipofectamine were mixed with 96µl Opti-MEM Medium in wells of a 6-well plate. 100µl of siRNA, diluted to 20nM in Opti-MEM Medium, were added and the mix was incubated for 15 minutes at RT. Meanwhile cells were trypsinized, counted and seeded at 75 000 cells/per well on top of the siRNA mixture. 24h after transfection the culture medium was changed.

Forward transfection:

The culture medium of the 6-well plates was changed 2h before transfection. 4µl Lipofectamine, diluted in 96-well Opti-MEM, were incubated for 15minutes at RT with 20nM siRNA in 100µl Opti-MEM and added into the culture medium of the cells. The following day a medium change was carried out.

Protein knockdown was checked by Western blot and cell proliferation was followed by the CSI until the cells reached confluence.

Materials	Company	Cat.No.
ON-TARGETplus siRNA EZH2	Dharmacon	J-004218-07
ON-TARGETplus SMART pool EZH2	Dharmacon	L-004218-00-0020
ON-TARGETplus Non-targeting Pool	Dharmacon	D-001810-10
Lipofectamine® RNAiMAX Reagent	Invitrogen	13778-150
Opti-MEM® Reduced Serum Medium, no phenol red	Gibco	11058-021

Table 14. Materials for siRNA transfection

Reverse transcription quantitative PCR (RT q-PCR)

Verification of EZH2 knockdown at the mRNA level and assessment of EZH2 target gene signature.

Preparation of complementary DNA (cDNA)

cDNA was prepared directly from cells cultured in 96-well plates using the Quiagen Fast lane Cell cDNA Kit according to the manufacturers instructions.

The medium of a 96-well plate was aspirated and cells were washed with 100µl/well FCW washing buffer in order to remove extracellular material secreted by living cells and intracellular material derived from dead or lysed cells. The washing buffer was discarded and 25µl/well FCP lysis buffer, stabilizing the cellular RNA and blocking inhibitors of reverse transcription, were added. The plate was shaken for 5-10 minutes at room temperature and either frozen at -80°C or directly used for cDNA synthesis.

Degradation of genomic DNA

All pipetting steps were carried out on ice. 4µl of the FCP lysates were transferred into a 96-well PCR Plate. For degradation of the genomic DNA 2µl/well gDNA wipeout buffer and 8µl/well RNAse-free water were added. To reduce pipetting mistakes, a master mix was prepared. The plate was sealed with an Eppendorf foil, shortly spinned down and incubated for 5 minutes at 42°C.

Reverse transcription

6µl of master mix (containing 1µl/well Quantiscript RT enzyme, 1µl RT primer mix, 4µl Quantiscript RT buffer [5x]) were added to each well. Per condition an extra well was prepared in which 1µl RNAse free H_2O was added instead of the RT enzyme. The resulting sample is a control in the final PCR reaction since no product can be yielded except if insufficiently degraded genomic DNA is still present. The reaction was incubated for 30 minutes at 42°C followed by 3 minutes at 95°C.

Materials	Company	Cat.No.
Fast lane Cell cDNA Kit (50)	Quiagen	215011

Table 15. Materials for cDNA synthesis

RT q-PCR

RT q-PCR was carried out with the Quiagen QuantiTect Multiplex PCR Kit according to the manufacturers instructions. For relative quantification of target gene amplification normalization to the housekeeping gene RNAse P was carried out by the $2^{-\Delta\Delta C}{}_T$ Method [60].

For each primer to be used in the PCR a separate master mix was prepared (12.5µl/well Quantitex Multiplex 2x Buffer, 1.25µl/well RNAse P primer, 1.25µl/well primer-mix, 8µl/well H_2O). 2µl of cDNA were pipetted to the well bottoms of a 96-well PCR plate in triplicates and 23µl of RT q-PCR master mix were added. PCR was carried out in an Agilent Technologies Stratagene MX3005P machine.

PCR conditions (normal two step PCR, FAM and HEX):

- 8 minutes 95°
- 45 cycles:
    - 45 seconds 94°C
    - 45°C 60°C

Materials	Company	Cat.No.
Quantitet Multiplex PCR Kit	Quiagen	204543
TaqMan® Rnase P Control Reagents VIC™	Applied Biosystems	4316844

Table 16. Materials for RT q-PCR

Primer	RefSeq	Cat.No.	Amplicon length	Assay location	Exon boundary
EZH1	NM_001991.3	Hs00940463_m1	57	1809	15-16
EZH2	NM_001203247.1	Hs01016789_m1	128	2121	16-17
EED	NM_003797.3	Hs00537777_m1	110	2021	5-6
SUZ12	NM_015355.2	Hs00248742_m1	84	1140	8-9
BRCA1	NM_007294.3	Hs01556193_m1	59	5698	21-22
CDKN2A	NM_000077.4	Hs00923894_m1	115	764	2-3
CHD1	NM_004360.3	Hs01023894_m1	61	284	2-3
DAB2IP	NM_032552.2	Hs00368995_m1	77	1154	6-7
EPHB6	NM_004445.3	Hs01071144_m1	58	3241	16-17
FOXC1	NM_001453.2	Hs00559473_s1	61	1605	1-1
ITGB2	NM_000211.3	Hs00164957_m1	76	566	4-5
PTEN	NM_000314.4	Hs02621230_s1	135	3337	9-9
TXNIP	NM_006472.3	Hs00197750_m1	81	592	1-2
WNT2	NM_003391.2	Hs00608224_m1	119	1152	4-5

Table 17. TaqManR Gene Expression Assays, Applied Biosystems

RESULTS

EZH2 is overexpressed in human cancer tissues

We searched the Boehringer Ingelheim in house database TANGO for relative expression levels of EZH2 in various normal (Figure 11A) and cancer tissues (Figure 11B). Values above 100 in Affymetrix mRNA hybridization assays indicate a high probability that EZH2 is expressed. In most normal tissues we found EZH2 relative expression values below 100. High relative EZH2 expression levels in normal tissues were observed in some tissues including Thymus and Testis. As opposed to normal tissues, we found relative EZH2 expression levels elevated in all cancer tissues analyzed in the database, as indicated in Figure 11B.

A

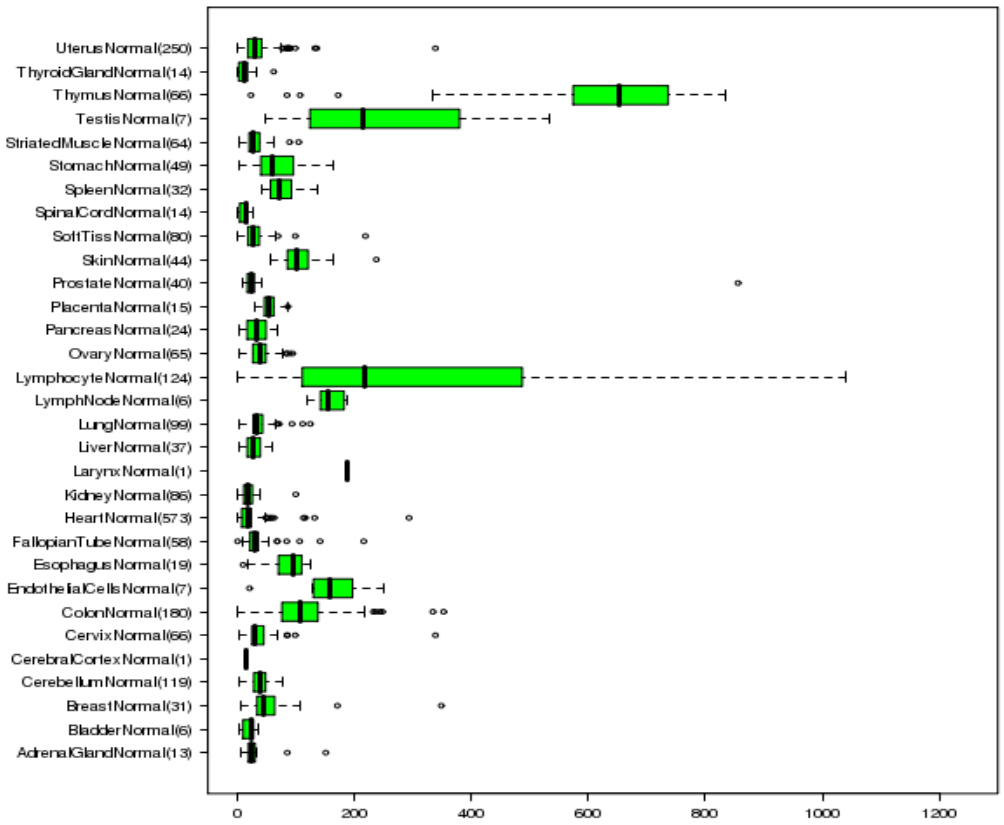

B

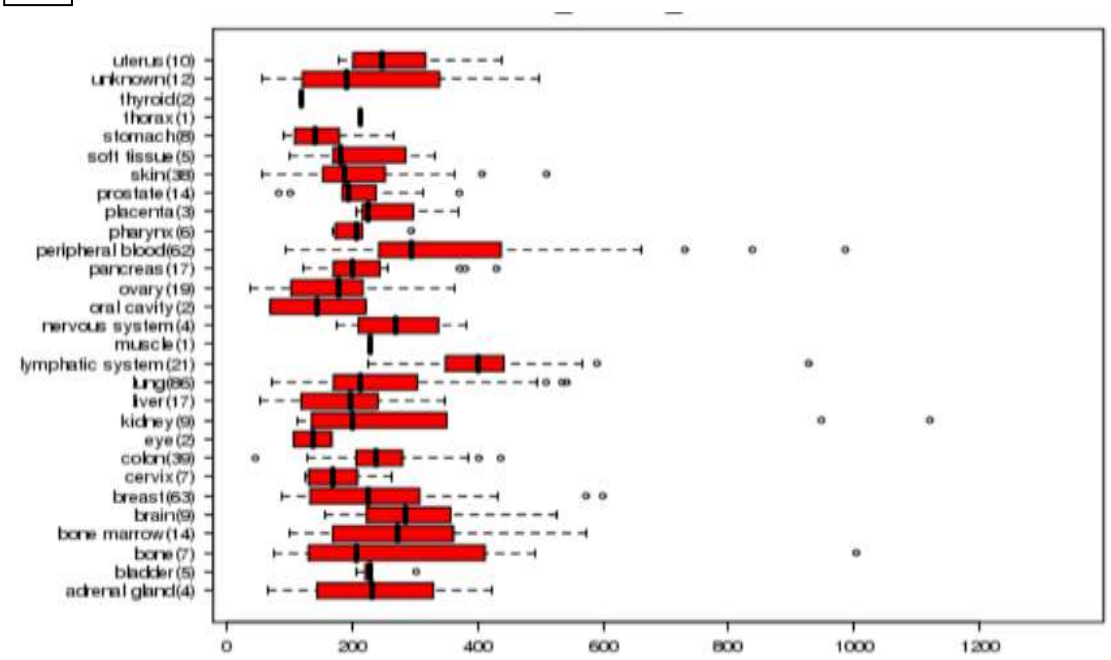

Figure 11. Relative EZH2 expression levels in normal and cancer tissues. (A) Relative expression levels of EZH2 in human normal tissues. **(B)** Relative EZH2 expression levels in human cancer tissues. The Expression levels were derived from the in-house database TANGO which is based on affymetrix microarray hybridization of mRNA of a broad panel of human normal and cancer tissues. Values above 100 indicate a high probability that the protein in question is expressed.

EZH2 is overexpressed in a broad panel of human cancer cell lines

To validate the data obtained in tissues, we analyzed the expression levels of EZH2 and its homolog EZH1 in a panel of different human cancer cell lines by using the Boehringer Ingelheim in-house database TANGO. In Figure 12 cell lines were sorted on the basis of rising EZH2 mRNA expression levels.

In Table 18, we also reported information on EZH2 amplification or mutation on the above-mentioned cell lines using the TANGO database.

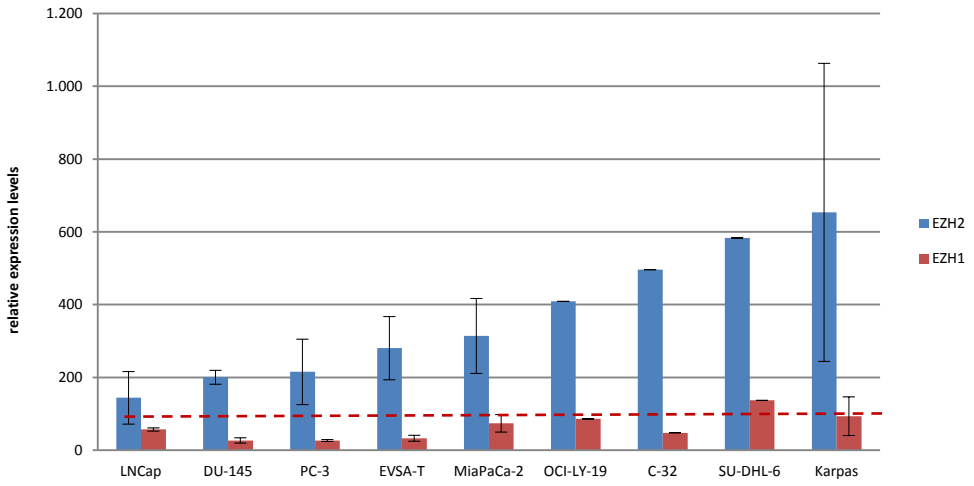

Figure 12. Relative expression levels of EZH2 and EZH1 in a panel of human cancer cell lines. The Expression levels were derived from the in-house database TANGO which is based on affymetrix microarray hybridization of mRNA of a broad panel of human cancer cell lines. High standard deviations are due to discrepancies of results derived from different chips. Values above 100 (marked by the red dashed line) indicate a high probability that the protein in question is expressed. For information on cell lines consult **Table 18**.

Cell line	Tumor type	Organ	TANGO
EVSA-T	carcinoma	breast	High EZH2, low EZH1
C32	melanoma	skin	EZH2 amplification: 3.8
MIA PaCa-2	carcinoma	pancreas	Deletion of the H3K27 demethylase UTX
OCI-LY-19	non hodkin's B-cell lymphoma	peripheral blood	EZH2 wild type
Karpas-422	non hodkin's B-cell lymphoma	peripheral blood	EZH2 Tyr641N point mutation
SU-DHL-6	non hodkin's B-cell lymphoma	lymphatic system	EZH2 Tyr641N point mutation
DU 145	carcinoma	Prostate	Androgen insensitive
PC-3	adenocarcinoma	Prostate	Androgen insensitive
LNCaP.FGC	adenocarcinoma	Prostate	Androgen sensitive

Table 18. List of cell lines used for knockdown experiments. The Boehringer Ingelheim in-house database TANGO was used to define the genetic backgrounds of the utilized cells.

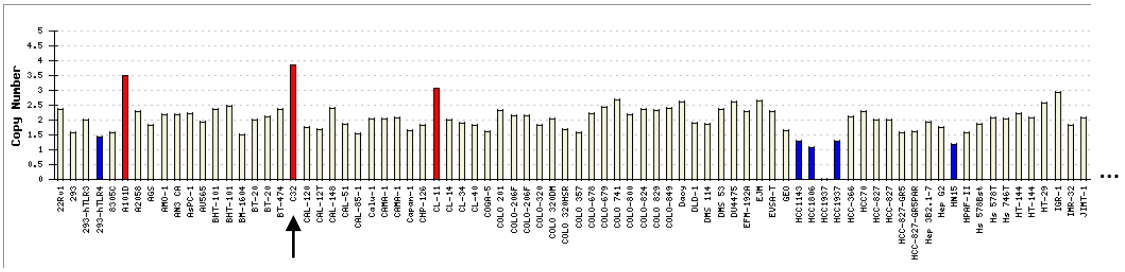

Figure 13. Amplification of EZH2 in C32 cells. The Boehringer Ingelheim in-house database TANGO provides sequencing data of an extensive number of cell lines. The graph shows copy numbers of EZH2. White bars represent the normal state of two copies per cell line. Red bars indicate gene amplification while blue bars show gene deletion. The arrow marks the position of the C32 cell line.

Verification of data derived from the TANGO database by Western blot

Whole cell lysates of the cell lines shown in Table 18 were analyzed by Western blot.

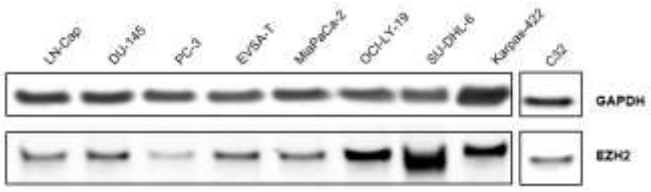

Figure 14. Verification of EZH2 protein expression levels by Western blot. Total cell lysates of a panel of human cancer cell lines were analyzed by western blot.

The Western blot data confirm the trend for EZH2 expression as predicted by our in silico analysis. The PC3 cells, which show the lowest EZH2 protein level, have also highly variable levels of EZH2 mRNA as indicated in Figure 14. Detection of EZH1 was not possible by Western Blot due to the lack of a good working anti-EZH1 antibody. We tested 4 different EZH1 antibodies (Table 13), but failed to detect any differences in band intensity in knockdown cells as compared to the controls (shRNA knockdown experiments, knockdown proven by RT q-PCR). Increasing the amount of loaded lysates, as suggested by Margueron and colleagues [22], did not improve the outcome (data not shown). EZH1 levels could therefore be analyzed only by RT q-PCR.

Study of the role of EZH2 in human cancer cell proliferation

To validate the role of the H3K27 methyltransferase EZH2 in cancer cell proliferation, we knocked down the protein in various human cancer cell lines in which EZH2 has been found overexpressed, amplified or mutated. To knock down EZH2 expression we used small-interfering siRNAs or short hairpin shRNA lentiviral particles for short and long term knock down experiments respectively.

Knockdown of EZH2 by siRNA

Overexpression of EZH2 correlated with poor clinical prognosis has been frequently reported in breast and prostate cancer [13]. Therefore, we first knocked down EZH2 by siRNA in EVSA-T breast cancer cells. According to our in silico analysis EVSA-T cells have high levels of EZH2, while they express only low levels of its homolog EZH1.

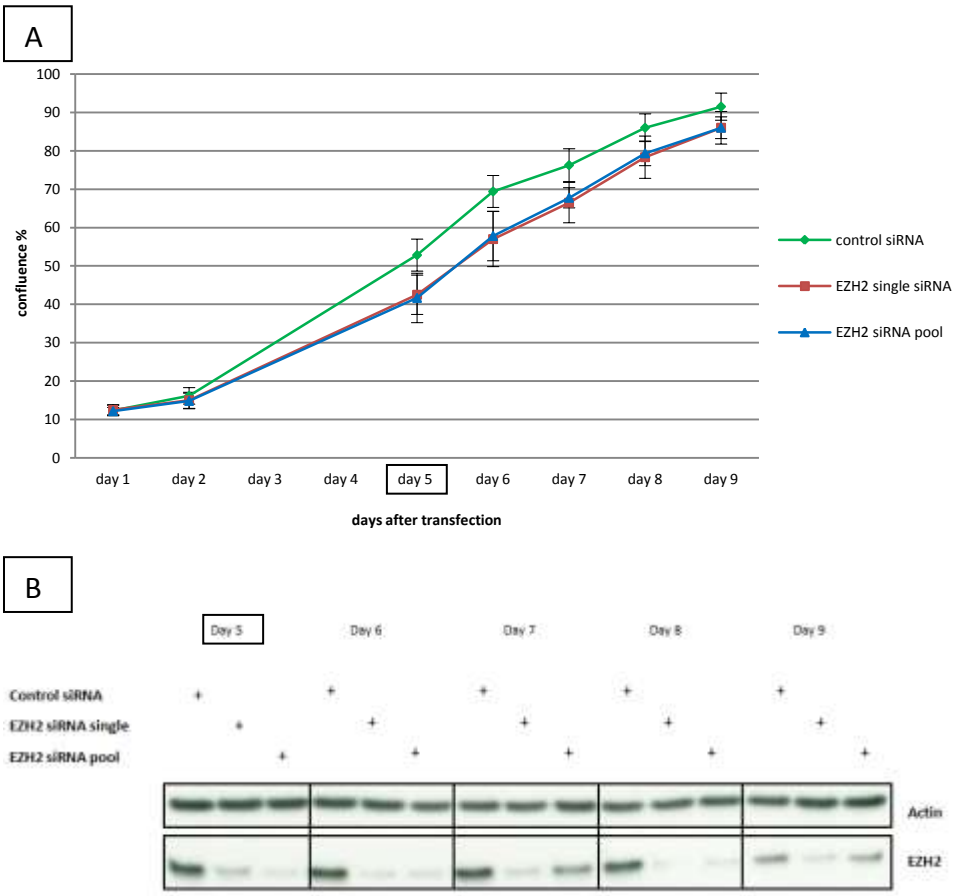

Figure 15. Knockdown of EZH2 by siRNA. EVSA-T breast cancer cells were reverse transfected with a single antiEZH2 siRNA, an EZH2 siRNA pool and a non targeting siRNA pool. **(A)** Cell proliferation was followed by daily measurement of confluence with the Clone Select Imager (CSI) from the first day of plating and transfection. Five days after transfection cells were re-transfected to maintain EZH2 knockdown. Mean confluence values were calculated of 6 wells measured (from day 5 cells of one well per condition were daily lysed for Western blot analysis). Error bars represent SD. **(B)** Verification of protein knockdown by Western blot before re-transfection (day 5) and the following 4 days. Results of 1 representative experiment (n=3).

Cells were transfected as described in Methods using single specific EZH2 siRNA oligo, a pool of specific EZH2 siRNAs or control siRNAs and cell proliferation was followed by daily measuring cell confluence with the Clone Select Imager (CSI). Five days after plating we observed 20% reduced proliferation of EZH2 knockdown cells as compared to the control. We found no difference in cell proliferation when we used a single EZH2 siRNA oligo or an EZH2 siRNA pool. Consistent with this, Western blot analysis showed an efficient knockdown of EZH2 protein using both approaches, but we could not detect significant changes in the mono-, di-, and trimethylation of H3K27 (data not shown). Due to the relatively high number of cells which had to be used in the siRNA experiments, cells reached a confluence of 80% already 7 days after plating and this did not allow us to follow cell proliferation and methylation status at H3K27 for a longer time.

Knockdown of EZH2 by shRNA

To determine the effects of long-term EZH2 knockdown on cell proliferation as well as on the biomarker status, cells were transduced with lentiviruses carrying short hairpin RNA (shRNA) against EZH2. The stable integration of lentivirus into the genome of the tumor cells allowed us to observe the effects of a prolonged knockdown of EZH2 over many cell divisions. Selection of cells which had integrated the virus into their genome by puromycin also allowed experiments with a quite homogenous cell population of EZH2 knockdown cells.

Determination of optimal puromycin concentrations for selection

Before transducing cells with lentivirus, we determined the optimal puromycin concentrations for selection in every cell line. For efficient selection the minimal puromycin concentration that completely kills all non transduced cells after 3 to 5 days was recommended by the manufacturer of the shRNA lentiviruses. Table 19 summarizes all the puromycin concentrations per cell line used in these studies.

Cell line	Puromycin concentration used
EVSA-T	4µg/ml
C32	4µg/ml
MIA PaCa-2	4µg/ml
OCI-LY-19	2µg/ml
Karpas-422	2µg/ml
SU-DHL-6	2µg/ml
DU 145	2µg/ml
PC3	2µg/ml
LNCaP.FGC	4µg/ml

Table 19. Optimal puromycin concentrations determined for different cancer cell lines. Cells were seeded in a 96-well plate and treated with different concentrations of puromycin (0, 0.5, 1, 2, 4, 8µg/ml) in triplicates 1 day after plating. 3 days later cell metabolism was measured with an Alamar Blue assay and the minimum puromycin concentration to kill all non transduced cells was determined.

Validation of EZH2 shRNA viruses

To identify the most potent EZH2 lentivirus we transduced EVSA-T cells with 4 different lentiviral constructs and analyzed cell proliferation as well as EZH2 protein knockdown.

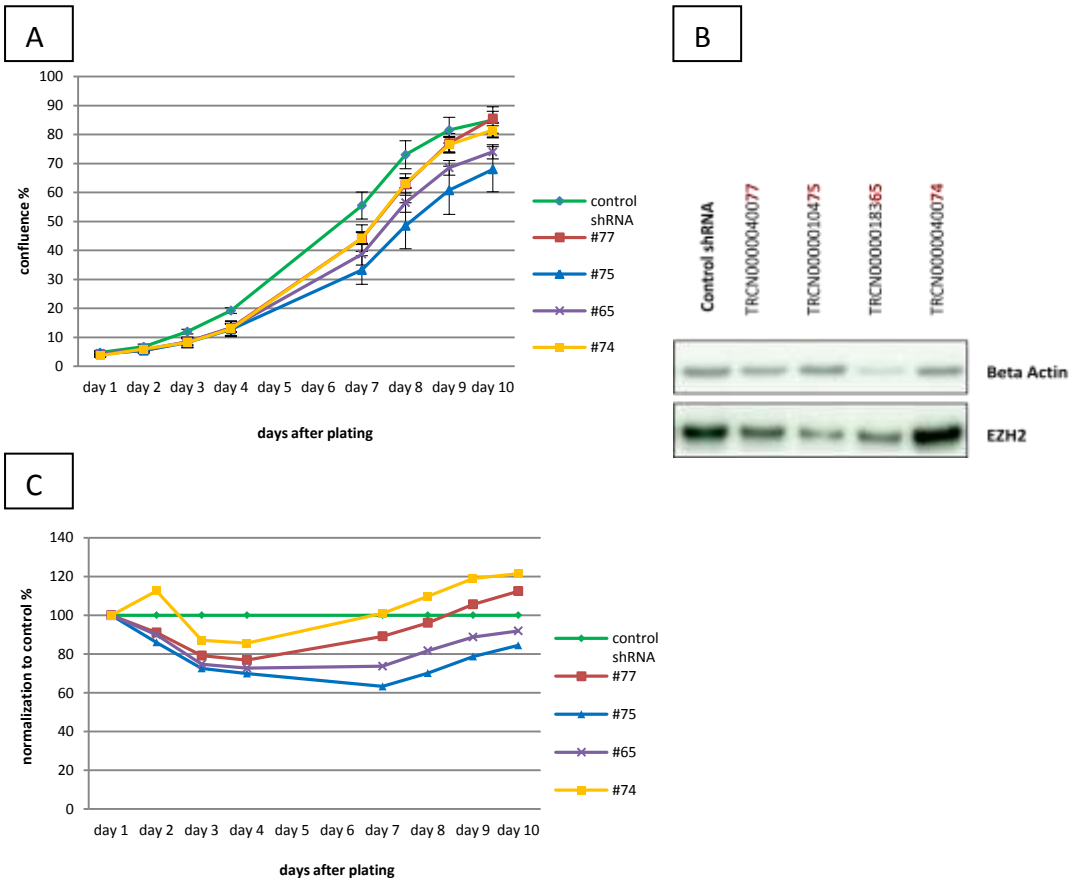

Figure 16. Validation of shRNA lentiviruses. (**A)** Cells were transduced with a non targeting control virus and 4 different EZH2 shRNA viruses. 5 days after viral transduction the cells were seeded at 1000cells/well in triplicates in a 96-well plate and the confluence of individual wells was measured on a daily basis by the Clone Select Imager (CSI). (**B)** Western Blot analysis of EZH2 knockdown 9 days after transduction, corresponding to 4 days after plating (**C)** All confluence values were normalized to the first day of confluence measurement and then calculated in percent of the non targeting control construct for every time point.

EVSA-T cells were transduced with four different EZH2 shRNA viruses (#77, #75, #65, #74) and a control lentivirus coding for a non targeting shRNA. All the viral constructs carried the puromycin resistance gene Puromycin N-acetyl Transferase (PAC). Upon addition of puromycin into the growth medium of cells two days after transduction, only cells which had incorporated the lentivirus into their genome could survive, since puromycin inhibits mRNA translation [56, 57].

Five days after viral transduction the cells were seeded at 1000cells/well in a 96-well plate and cell proliferation was followed for 10 days by the Clone Select Imager (CSI) which measured cell confluence. As shown in Figure 16A (and in its normalization in Figure 16C), construct number #75 showed the highest efficiency in proliferation

reduction with a maximum of 40% reduced proliferation at day 7 as compared to cells transduced with the non targeting shRNA virus. Cells transduced with the non targeting control shRNA construct reached a confluence of 80% at day 9 (Figure 16A).

To determine the knockdown of EZH2, we analyzed cell lysates by Western blot. The results of this analysis are shown in Figure 16B. We found a good correlation between the ability of the lentivirus to block EZH2 expression and its inhibitory effect on cell proliferation. Construct number #75 led to the most efficient knockdown as compared to EZH2 levels of cells transduced with the non targeting control virus. Construct number #74 which did not show an effect on cell proliferation also had no effect on EZH2 protein levels. Weak effects of the constructs number #77 and #65 were also reflected in the lower degree of EZH2 knockdown. These findings confirm specific effects of EZH2 shRNA knockdown on cell proliferation.

The experiment was repeated for the viruses showing the strongest effect on cell proliferation and EZH2 knockdown with reproducible results (data not shown).

The lentiviral construct #75 was used in all further experiments to study the involvement of EZH2 in cancer cell proliferation.

Effect of different cell densities on cell proliferation differences

To test the prolonged effect of EZH2 knockdown, EVSA-T cells were seeded at different cell densities, infected with lentivirus #75, as previously described, and proliferation was followed by the Clone Select Imager (CSI) until the cells reached 80-100% confluence.

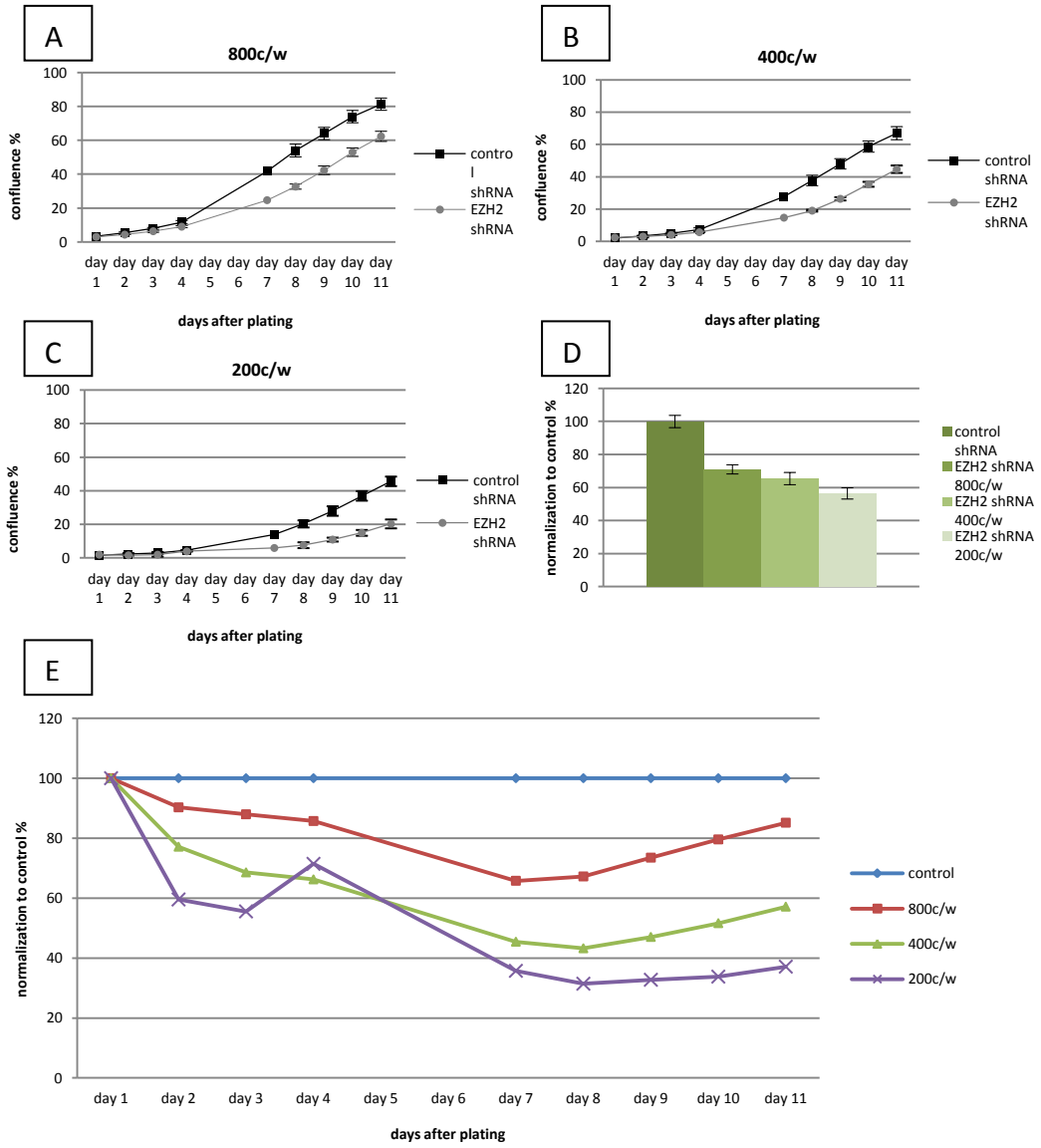

Figure 17. Reduced proliferation in EVSA-T breast cancer cells dependent on cell number. Cells were transduced with a non targeting control virus and an EZH2 shRNA virus. 5 days after viral transduction the cells were seeded at **(A)** 800, **(B)** 400 and **(C)** 200 cells/well in triplicates in a 96-well plate and the confluence of individual wells was measured on a daily basis by the Clone Select Imager (CSI). (**D)** Determination of cell proliferation by the metabolic Alamar Blue assay 9 days after plating. The values of cells transduced with EZH2 virus were calculated in percent of the non targeting control cells. **(E)** All confluence values were normalized to day 1 after plating and calculated in percent of the respective control cells for every time point.

As shown in Figure 17A-C and in its quantification in Figure 17E, EVSA-T cells transduced with EZH2 lentivirus show reduced proliferation as compared to the control. Interestingly, we noticed that the inhibitory effect on cell proliferation was stronger

when cells were plated at lower densities. This effect was accompanied by a specific and strong decrease of EZH2 protein level in cells transduced with EZH2 lentivirus as demonstrated by WB and RT qPCR data in Figure 18A-B. Of note, EZH1 mRNA level remained unchanged (Figure 18B). Importantly, for the first time we observed that cells transduced with EZH2 lentivirus had a significantly lower trimethylation level of H3K27 as compared with cells transduced with control lentivirus.

In addition, we wanted to confirm these findings by measuring cell proliferation using a different read-out. To this end, cells were transduced with EZH2 or control lentivirus and cell proliferation was monitored by the metabolic Alamar Blue assay. As shown in Figure 17D, the Alamar Blue assay confirms a reduction in metabolism of EZH2 knockdown cells as compared to the control 9 days after plating. It should be noted that the effect of different cell densities was not as dramatic as observed for measurement of cell confluence.

Determination of cell proliferation differences following the knockdown of EZH2 was therefore always carried out by both methods in all following experiments.

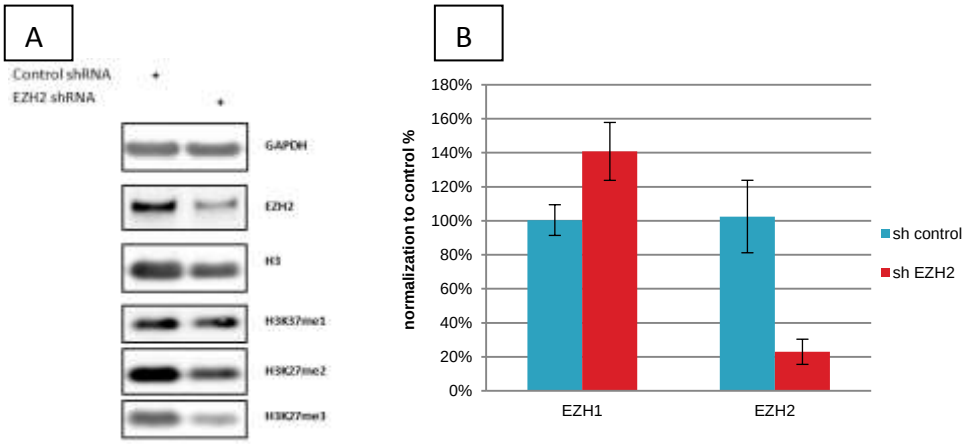

Figure 18. Confirmation of EZH2 knockdown in EVSA-T breast cancer cells. (A) Cells were seeded in 12-well plates at 1000 cells/well and lysed 21 days after transduction. EZH2 protein level as well as biomarker status were analyzed by western blot. **(B)** Cells were seeded in 96-well plates at 800 cells/well and analyzed by RT q-PCR 14 days after transduction. mRNA levels were normalized to the housekeeping gene RNaseP and calculated in percent of the control cells.

Effect of EZH2 knockdown in cell lines with an EZH2 point mutation

Next, we analyzed the effect of EZH2 knockdown in Karpas-422 cells with a heterozygous point mutation in the histone methyltransferase at tyrosine 641 to asparagine (N). The wild type EZH2 catalyzes zero to monomethylation of H3K27, while the mutated enzyme was reported to have increased catalytic activity for the mono- to dimethylation and the di- to trimethylation of H3K27 [54]. This increased activity leads to higher trimethylation level of EZH2 target promoters and aberrant gene silencing. Since the EZH2 lentivirus used for the knockdown recognized the 3' UTR of the EZH2 mRNA transcript, we expected an equal downregulation of the wild type and the mutated EZH2.

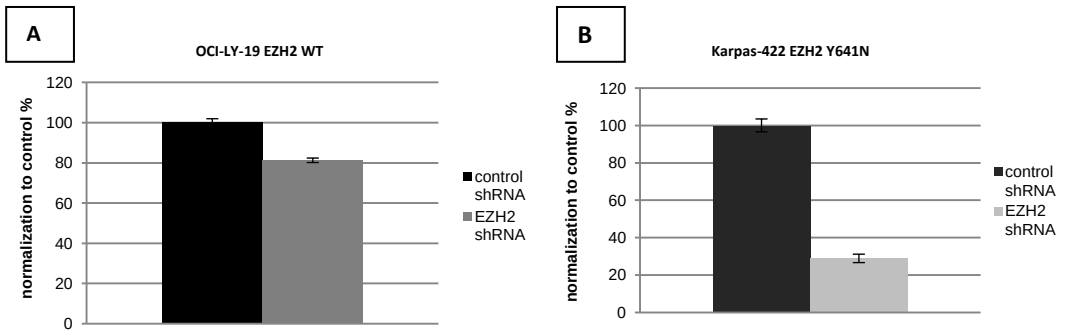

Figure 19. Reduced metabolic activity in cells with an EZH2 point mutation. (A) OCI-LY-19 EZH2 WT control cells and **(B)** Karpas-422 EZH2 Y641N cells were transduced with EZH2 shRNA and a non targeting control shRNA and seeded in 96-well plates 5 days after transduction. Cells were seeded at 5000 cells/well in triplicates and an Alamar Blue assay was performed 7 days after plating. Metabolism values of EZH2 knockdown cells were calculated in percent of cells transduced with the non targeting control shRNA.

As already observed for adherent cells, differences in proliferation were in most cases obvious only after some days when cell numbers started to diverge. 7 days after transduction the EZH2 point mutated Karpas-422 cells showed almost 80% reduced proliferation of EZH2 shRNA transduced cells while the OCI-LY-19 cells showed only 20% reduced proliferation of EZH2 as compared to control cells.

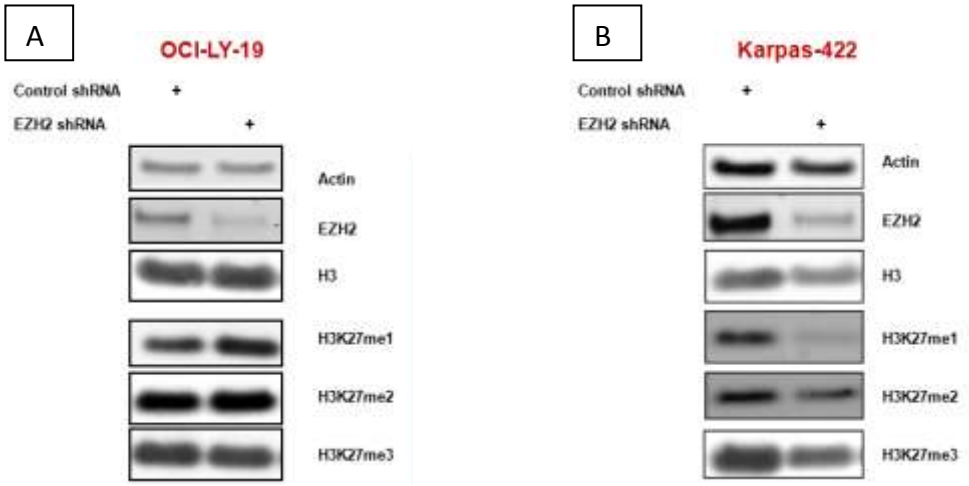

Figure 20. Verification of EZH2 knockdown in B-cell lymphoma cells with (A) wild type EZH2 and (B) an EZH2 point mutation. 12 days after transduction cells were lysed and EZH2 protein expression as well as biomarker status were analyzed by western blot.

EZH2 was efficiently knocked down in Karpas-422 and OCI-LY-19 B-cell lymphoma cells. Karpas-422 cells have a heterozygous mutation in EZH2 which is knocked down to the same extent of the wt allele. We observed slightly reduced trimethylation of H3K27 in both cell lines as a consequence of EZH2 protein knockdown.

Reduced proliferation of EZH2 amplified cells

According to the database TANGO C-32 melanoma cells have an EZH2 amplification of 3.8. Therefore, we set out to investigate the role of EZH2 in the proliferation of these cells.

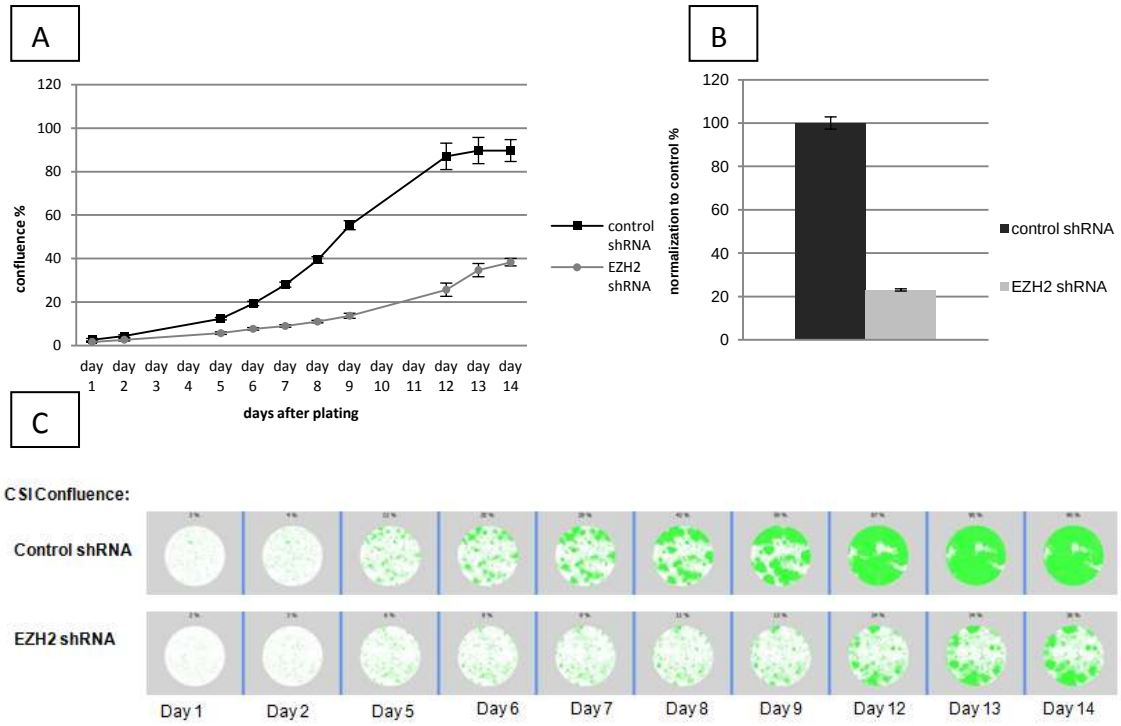

Figure 21. Reduced proliferation in C-32 melanoma cells with an EZH2 amplification of 3.8. (A) Cells were transduced with a non targeting control virus and an EZH2 shRNA virus. 5 days after viral transduction the cells were seeded at 800cells/well in triplicates in a 96-well plate and the confluence of individual wells was determined on a daily basis by the Clone Select Imager (CSI). (**B)** Determination of cell proliferation by the metabolic Alamar Blue assay 13 days after transduction. The values of cells transduced with EZH2 virus were calculated in percent of the non targeting control cells. (**C)** Daily measurement of confluence by the CSI. One well per triplicate is shown.

C-32 melanoma cells were transduced with EZH2 lentivirus and cell proliferation was followed by the CSI. As shown in Figure 21A and in the schematic representation in Figure 21C, cells transduced with EZH2 specific lentivirus showed a decreased proliferation compared to the non targeting control lentivirus over a period of 14 days. We confirmed this observation also by measuring cell proliferation using the Alamar Blue assay (see Figure 21B).

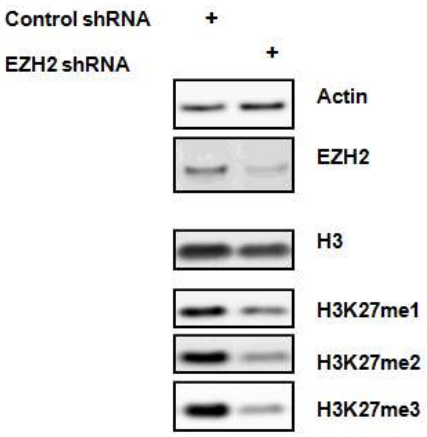

Figure 22. Western Blot analysis of EZH2 knockdown and H3K27 methylation status in C-32 cells. Cells were seeded at 1000cells/well in a 12-well plate and lysates were prepared 14 days after plating. EZH2 knockdown as well as the biomarker status were analyzed by western blot.

To prove that the inhibition of cell proliferation in C32 cells is due to EZH2 knockdown, we analyzed the EZH2 protein levels by Western Blot in C32 cells transduced with EZH2 and control lentivirus. Figure 22 shows that EZH2 protein level as well as H3K27 trimethylation was significantly lower in cells transduced with EZH2 particles compared with the non-targeting control.

Reduced proliferation in UTX deleted MiaPaca-2 cells

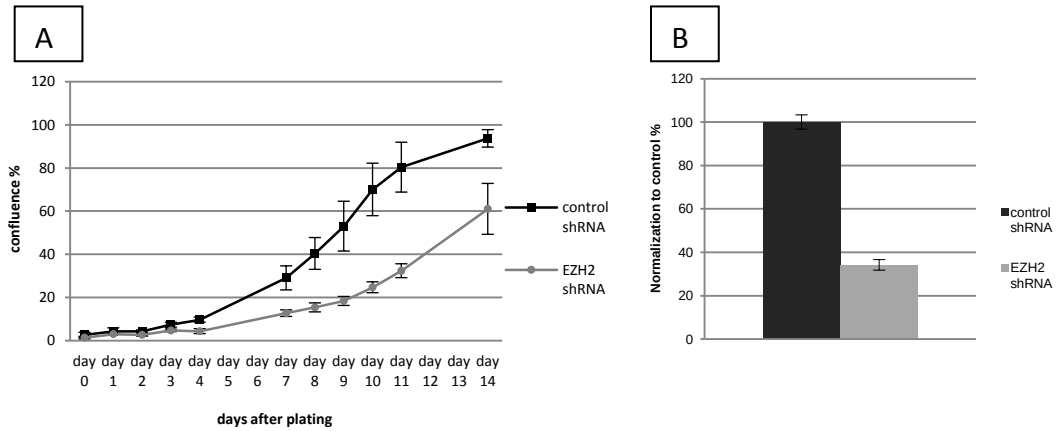

Figure 23. Reduced proliferation in UTX deleted MiaPaCa-2 Pancreas carcinoma cells. (A) Cells were transduced with a non targeting lentivirus control and an anti EZH2 lentivirus. 5 days after viral transduction the cells were seeded at 200cells/well in triplicates in a 96-well plate and the confluence of individual wells was measured on a daily basis by the Clone Select Imager (CSI). (**B)** Determination of cell proliferation by the metabolic Alamar Blue assay 13 days after

transduction (8 days after plating). The values of cells transduced with EZH2 virus were calculated in percent of the non targeting control cells.

UTX is the demethylase which removes the methyl groups from the Lysine-27 of the histone H3. Van Haaften and colleagues report that the pancreatic cancer cell line MiaPaCa-2 has a homozygous deletion across all coding exons of the H3K27 demethylase UTX [12]. This was verified by the database TANGO and by in-house experiments (data not shown).

A deletion of an important H3K27 demethylase leads to increased H3K27 trimethylation and thereby target gene repression. We reasoned that these cell lines would be more sensitive to changes in EZH2 protein levels, thus representing one of the ideal models to study the effect of EZH2 knock down on cell proliferation. To this aim, MiaPaCa-2 cells were transduced with EZH2 or control lentivirus and cell proliferation was followed over a period of 14 days by CSI or 8 days after transduction by Alamar Blue assay.

As shown in Figure 23A-B, using both read-outs, we noticed that cells transduced with the anti EZH2 lentivirus showed reduced proliferation compared with cells transduced with control lentivirus. This inhibitory effect on cell proliferation was accompanied by marked decrease of EZH2 protein as well as H3K27 trimethylation levels, as indicated in Figure 24A. Interestingly, we noticed a reproducible increase of EZH1 mRNA levels in EZH2 lentivirus transduced cells (Figure 24B).

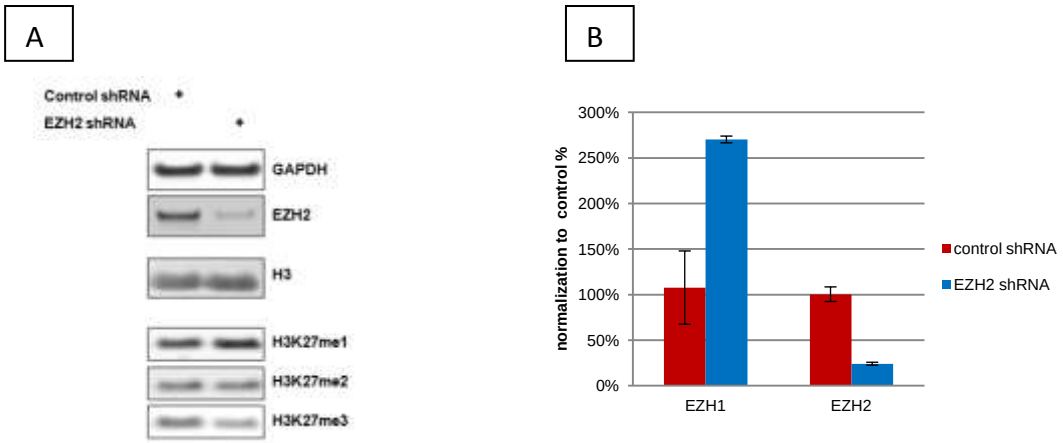

Figure 24. Verification of EZH2 knockdown in MiaPaCa-2 cells. (A) Western Blot analysis of EZH2 knockdown and H3K27 methylation status 14 days after transduction with anti EZH2 shRNA lentivirus. (**B)** RT q-PCR Analysis of EZH1

and EZH2 levels 14 days after transduction with anti EZH2 lentivirus (8 days after plating). The values were normalized to the housekeeping gene RNaseP and calculated in percent of the control shRNA cells.

Effect of EZH2 knockdown in prostate cancer cells

The DU-145 and PC3 cells are androgen insensitive prostate cancer cell lines derived from metastases to the brain and to the bone respectively. Both cell lines express neither androgen receptor (AR) nor prostate-specific antigen (PSA) [49]. The LNCaP.FGC cell line is sensitive to androgens and was derived from a lymph node metastasis. It expresses AR and PSA [49]. EZH2 expression levels were reported to be elevated in hormone refractory, metastatic prostate cancer and predictive for cancer outcome [45, 46]. We therefore were interested in the effects of EZH2 knockdown on these three prostate cancer cell lines.

Androgen insensitive prostate cancer cells: PC3

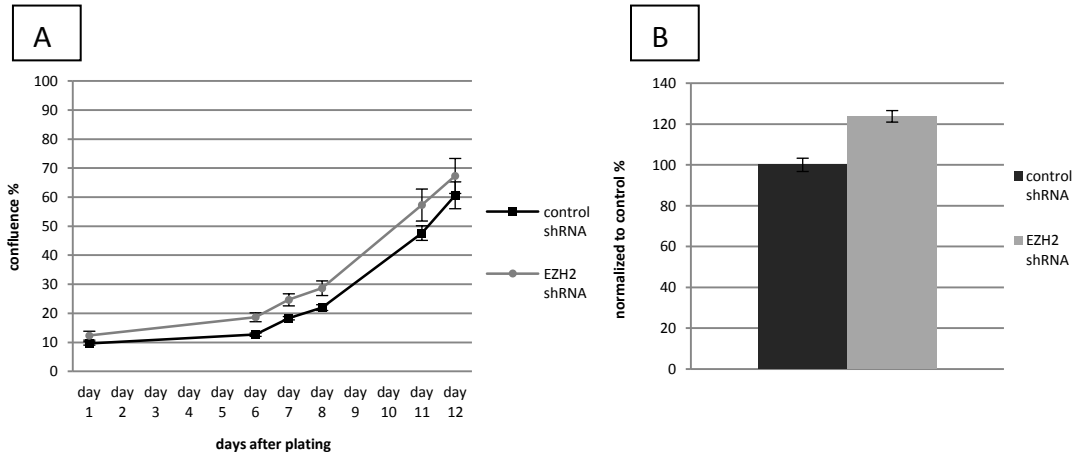

Figure 25. Unchanged proliferation of PC3 prostate cancer cells after lentiviral knockdown of EZH2. Cells were transduced with an anti EZH2 shRNA and a non targeting control shRNA. Five days after transduction the cells were seeded in triplicates at 1600 cells/well in a 96-well plate. **(A)** Cell proliferation was followed by measuring confluence on a daily basis by the CSI. **(B)** 13 days after transduction a metabolic Alamar Blue assay was carried out to determine cell proliferation. Metabolic activity was calculated in percent of the control cells.

Androgen insensitive PC3 prostate cancer cells, transduced with an EZH2 lentivirus, did not show reduced proliferation as compared to control shRNA cells. Daily measurement of confluence by the Clone Select Imager even showed a faster increase in confluence for EZH2 knockdown cells (Figure 25A). The Alamar Blue assay 13 days after transduction

(corresponding to 8 days after plating) confirms a 20% higher metabolic activity of EZH2 knockdown cells as compared to control cells (Figure 25B).

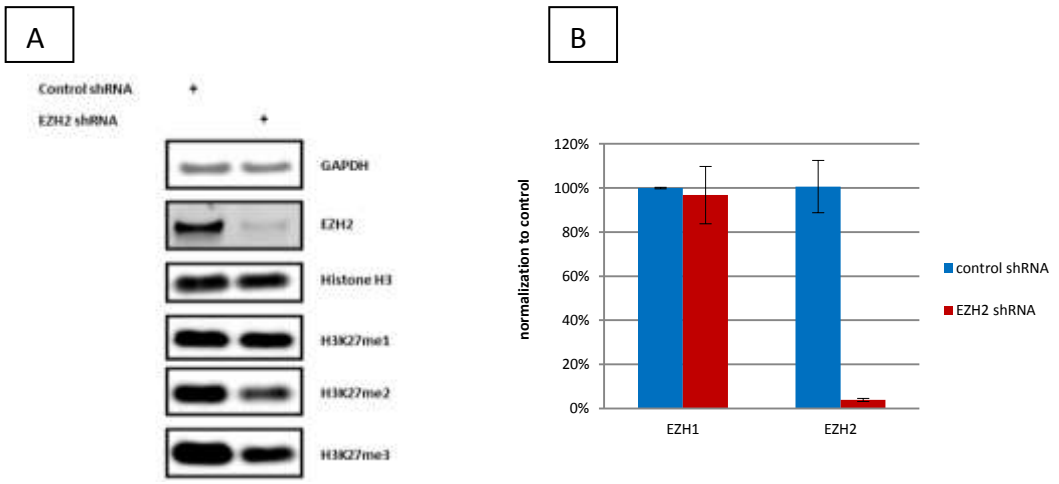

Figure 26. Verification of EZH2 knockdown in PC3 androgen insensitive prostate carcinoma cells. (A) Western Blot analysis of EZH2 knockdown 16 days after transduction with anti EZH2 shRNA lentiviruses. **(B)** RT q-PCR Analysis of EZH1 and EZH2 levels 14 days after transduction with anti EZH2 lentivirus. The values were normalized to the housekeeping gene RNaseP and calculated in percent of the control shRNA cells.

To confirm the knockdown of EZH2 in the cells used for the experiments shown in Figure 16, protein levels were analyzed by Western blot 11 days after plating. Despite the lack of proliferation reduction, we found a strong decrease of EZH2 mRNA and protein level (see Figure 26 right and left panel) followed by a reproducible 50% decrease of H3K27 trimethylation level.

Androgen sensitive prostate cancer cells: LNCaP.FGC

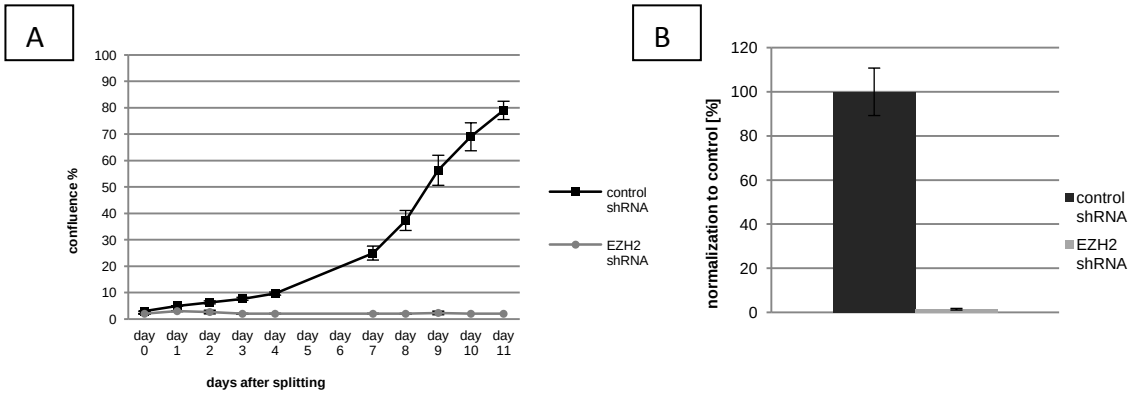

Figure 27. Proliferation arrest of LNCaP.FGC androgen sensitive prostate cancer cells upon EZH2 knockdown. (A) Cells were transduced with a non targeting control virus and an EZH2 shRNA virus. 5 days after viral transduction the

cells were seeded at 1600cells/well in triplicates in a 96-well plate and the confluence of individual wells was measured on a daily basis by the Clone Select Imager. **(B)** Determination of cell proliferation by the metabolic Alamar Blue assay. The values of cells transduced with EZH2 virus were calculated in percent of the non targeting control cells.

LNCaP.FGC cells are androgen sensitive prostate cancer cells. Cells were transduced with EZH2 or control lentivirus and cell proliferation was followed over a period of 11 days by CSI and Alamar Blue assay. The results reported in Figure 27A-B show that cells transduced with EZH2 stop proliferating as opposed to cells transduced with the non targeting control shRNA lentivirus. The Western blot and RT-PCR data in Figure 28 A-B indicate that i) EZH2 mRNA and protein levels were strongly reduced when cells were infected with EZH2 lentivirus and ii) EZH1 mRNA level was mostly unchanged. Due to the lack of protein extract because of the extent of inhibition of cell proliferation in this experiment, we were unable to confirm the concomitant decrease of H3K27 trimethylation level.

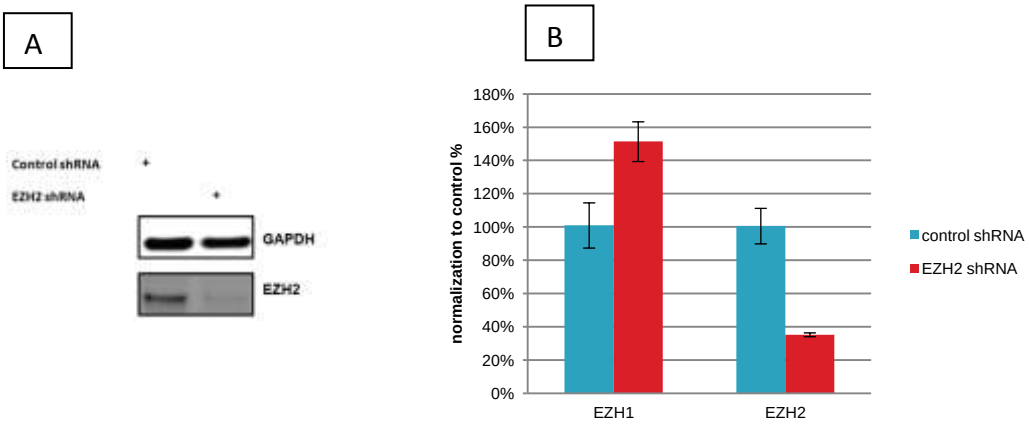

Figure 28. Verification of EZH2 knockdown in LNCap.FGC prostate carcinoma cells. (A) Western Blot analysis of EZH2 knockdown 14 days after transduction with anti EZH2 shRNA lentivirus. **(B)** RT q-PCR Analysis of EZH1 and EZH2 levels 14 days after transduction with anti EZH2 lentivirus. The values were normalized to the housekeeping gene RNAseP and calculated in percent of the control shRNA cells.

EZH2 knockdown reduces anchorage independent growth

We chose two cell lines, namely EVSA-T and MiaPaCa cells, to study the role of EZH2 in 3D cell proliferation. To this aim, we used a soft agar colony formation assay, which

measures the ability of cells to form colonies without a flat surface. In this assay, cells have to grow three dimensionally in the presence of contact inhibition and limited access to nutrients which mimics the growth conditions faced by cancer cells in vivo [49]

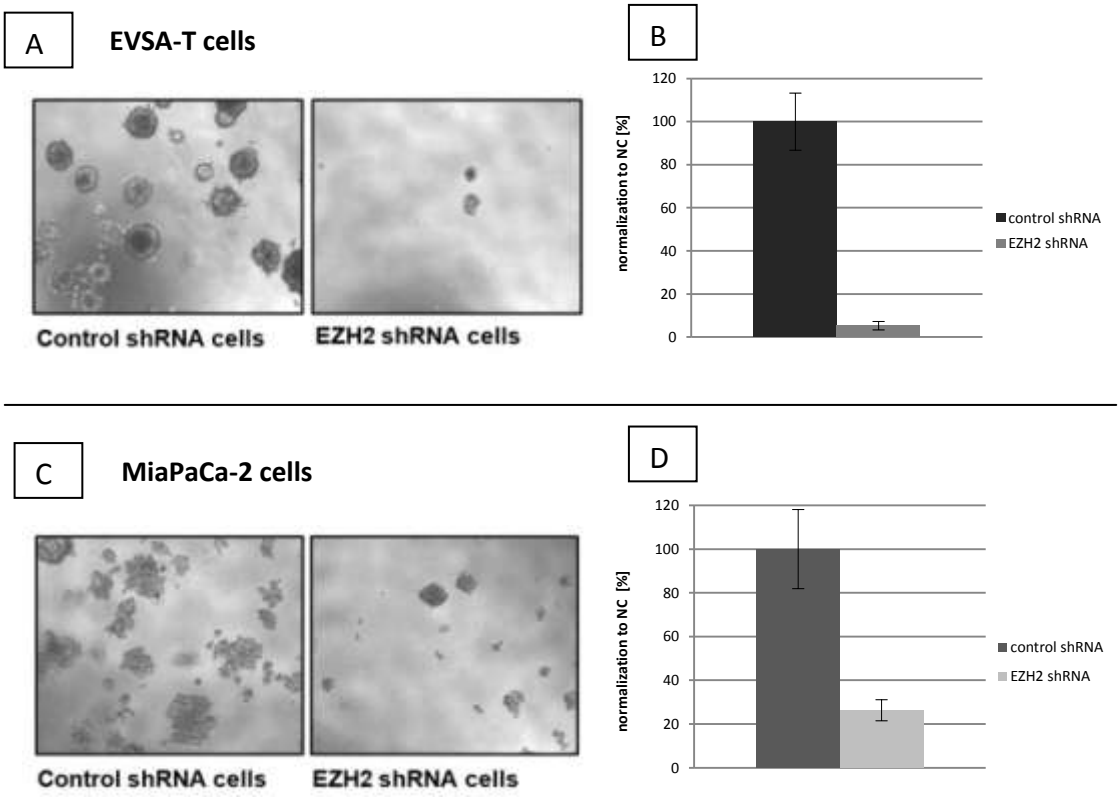

Figure 29. Reduced capacity to form colonies in soft agar of MiaPaCa-2 cells. Cells were embedded at 1000cells/well in medium containing 0.3% agarose at replicates of 5. **(A,C)** Cells were inspected microscopically on a daily basis and a picture was taken at the day of the metabolic Alamar Blue assay with a 2.5X objective. **(B,D)** To determine the number of viable cells per well proliferation was assessed 10 days after seeding by an Alamar blue assay. Metabolic values of EZH2 knockdown cells were calculated in percent of the control after subtraction of background values.

EVSA-T cells transduced with the non targeting control shRNA formed defined round colonies in the soft agar, while EZH2 knockdown cells formed only very small colonies, if any. The metabolic assay verified the observations made by microscopic inspection and shows a strong reduction of metabolic activity of >90% in EZH2 knockdown cells as compared to the controls. Similarly, in control shRNA-transduced MiaPaCa-2 cells, we could observe clearly visible colonies while in EZH2 knockdown cells we observed much

fewer and smaller colonies. Again the metabolic assay verified the microscopic observations and showed drastically reduced metabolism in wells with EZH2 knockdown cells as compared to the controls.

Repression of target genes by EZH2 knockdown

Several groups have shown that EZH2 activity affects different gene expression pathways. To test the effect of EZH2 knockdown on target gene repression, we selected 10 published EZH2 target genes and performed RT q-PCR in two selected cell lines (EVSA-T and MiaPaCa). The genes we chose to investigate are indicated in Table 20.

BRCA1	Homo sapiens breast cancer 1, early onset	[61]
CDKN2A	Homo sapiens cyclin-dependent kinase inhibitor 2A	[61-63]
CHD1	Homo sapiens cadherin 1, type 1, E-cadherin (epithelial)	[27, 64, 65]
DAB2IP	Homo sapiens DAB2 interacting protein	[61, 66]
EPHB6	Homo sapiens EPH receptor B6	[46]
FOXC1	Homo sapiens forkhead box C1	[67]
ITGB2	Homo sapiens integrin, beta 2 (complement component 3 receptor 3 and 4 subunit)	[46]
PTEN	Homo sapiens phosphatase and tensin homolog	[61]
TXNIP	Homo sapiens thioredoxin interacting protein	[68]
WNT2	Homo sapiens wingless-type MMTV integration site family member 2	[46]
	PRC2 Members:	
SUZ12	Homo sapiens suppressor of zeste 12 homolog	
EED	Homo sapiens embryonic ectoderm development	

Table 20. List of genes analyzed in RT q-PCR gene signature experiments. Changes in mRNA expression levels upon knockdown of EZH2 were tested in different cell lines. Underlined genes were derived from the EZH2 14-targetgene signature published by Yu and colleagues 2007.

Figure 30 shows the effect of EZH2 knockdown in the above-mentioned cell lines on the chosen target genes. In MiaPaCa-2 cells knockdown of EZH2 led to upregulation of other PRC2 members such as EED and SUZ12, indicating autoregulation of the complex components, as previously reported for some members of PRC1 [1]. We observed a 10-fold increase of TXNIP mRNA as compared to control cells. For EVSA-T cells, we could not detect any significant changes on the selected target genes 14 days after transduction with EZH2 shRNA.

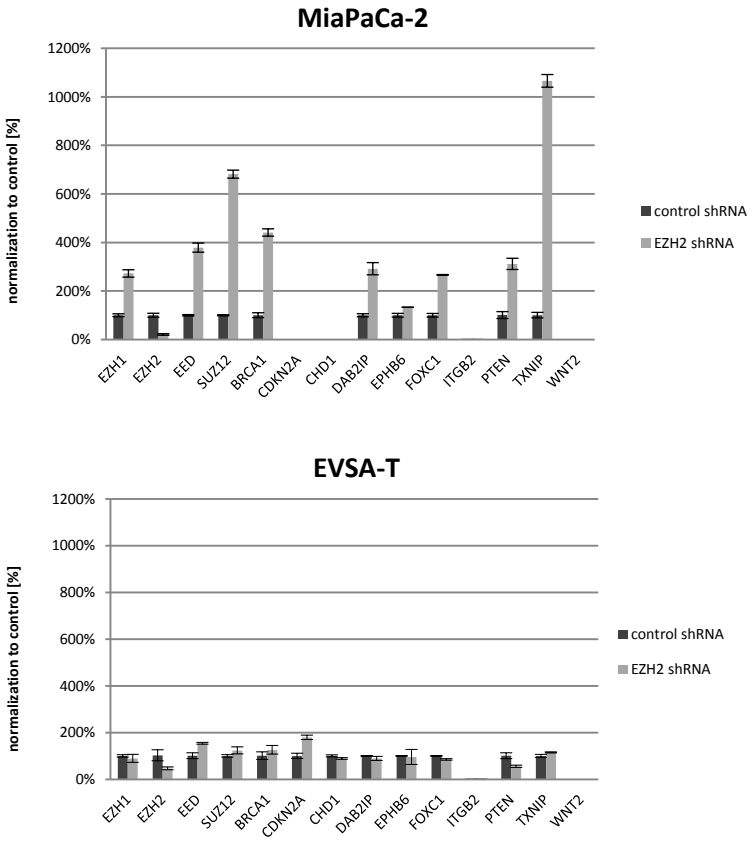

Figure 30. EZH2 target gene signature in MiaPaCa-2 cells (200c/w) and EVSA-T cells (800c/w). RT q-PCR Analysis of mRNA levels of 4 PRC2 members and 10 published EZH2 target genes 14 days after transduction with anti EZH2 lentivirus. The values were normalized to the housekeeping gene RNAseP and calculated in percent of the control shRNA cells. The cDNA prepared from the single wells was pooled before utilization in the various RT q-PCR reactions. Cells seeded at the same time as the respective growth curve experiments were used. Results of one representative experiment are shown (n=3 for MiaPaCa-2; n=2 for EVSA-T).

DISCUSSION

EZH2 is a histone methyltransferase frequently deregulated in cancer. Increased trimethylation of target genes leads to epigenetic repression of differentiation genes and an increased proliferative potential of cells reminiscent of stem cells. EZH2 was found to be predictive of cancer progression and patient outcome in many cancer types including prostate, breast, colorectoral cancer, etc. EZH2 also plays important roles in stem cell maintenance and proliferation. Cancer stem cells have been implicated in cancer recurrence and metastasis and are not responding to conventional therapy [43]. The hope for targeting proteins involved in epigenetic gene silencing in cancer is fuelled by the fact that epigenetic modifications are reversible.

For validation of EZH2 as a potential target in oncology, we chose cell lines with different genetic background of aberrant EZH2 expression. By this approach, we intended to identify a set of cancer types for which EZH2 inhibition might be a promising way of treatment. Recently, a group has elegantly discovered that heterozygous EZH2 mutations lead to increased di- and tri-methylation activity of H3K27, while the wild type methyltransferase is needed for the monomethylation reaction [54].

By searching the Boehringer Ingelheim in-house database TANGO, we found EZH2 overexpressed in cancer tissues as compared to normal tissues as previously reported [13]. We validated these findings by analyzing EZH2 protein levels in a panel of cancer cell lines by Western blot. To perform our studies which aimed at understanding the role of EZH2 in cancer cell proliferation, we chose cell lines in which EZH2 was i) highly overexpressed (EVSA-T) ii) subjected to gene amplification (C-32) iii) hyper-activated by activating mutations (Karpas-422) or iv) not counteracted because of inactivating mutations in the H3K27 demethylase UTX (MiaPaCa-2).

We first knocked down EZH2 by siRNA in EVSA-T breast cancer cells. By using the siRNA approach, although we observed a very potent knockdown of EZH2, proliferation of knockdown cells was not significantly reduced. Successively, we switched to lentiviral shRNA knockdown of EZH2. In this case, we noticed that EZH2 knockdown strongly

decreased cell proliferation using both 2D and 3D cell proliferation assays as shown for example in Figure 17 and in Figure 29 (A+B). Interestingly, we observed that this effect was dependent on cell density (Figure 17). To strengthen the nature of our observations, we followed cell proliferation by a confluence based assay and a metabolism based cell proliferation assay. Both approaches led us to the conclusion that EZH2 presence is necessary for cell proliferation in breast cancer EVSA-T cells. In addition, we did not observe any functional compensation by EZH1 as its mRNA levels were unchanged up to 21 days after EZH2 knockdown (Figure 18B).

In EZH2 amplified C32 melanoma cells we observed 60% difference in confluence 9 days after plating and 80% difference according to the metabolic assay 8 days after plating. EZH2 knockdown was accompanied by a strong decrease of H3K27me3 levels as well as a marked decrease of H3K27 mono- and di-methylation.

MiaPaCa-2 pancreas carcinoma cells with a deletion of the H3K27 demethylase UTX also reproducibly show a 60% reduced proliferation in both cell proliferation assays accompanied by a 50% reduction of global H3K27me3 levels. Importantly, EZH2 knockdown also strongly affected the ability of these cells to grow in 3D as shown in Figure 29 (C+D). Interestingly, we found a reproducible upregulation of EZH1 to 270% of the control when EZH2 was knocked down in these cells. This result suggests a possible compensatory mechanism in the function of these two enzymes in these cells. Future studies with double EZH2 and EZH1 knock down should clarify whether the upregulation of EZH1 upon EZH2 knockdown is part of a compensatory mechanism in these cells to counteract the loss of EZH2.

We also performed knockdown experiments on B-cell lymphoma cells with a mutation in tyrosine 641 to asparagine. Affymetrix expression data derived by the TANGO database indicated very high overall expression levels of EZH2 in the three B-cell lymphoma cell lines (see Figure 12). We hypothesized that cells with a hyperactivated EZH2 function should be especially susceptible to EZH2 knockdown. Interestingly we found that the Karpas-422 cells with an EZH2 Y641N mutation showed 70% reduced proliferation as compared to the EZH2 wild type OCI-LY-19 cells with only 20% reduced metabolic

activity. The growth type of the cells in suspension did not allow daily measurement of cell confluence. In both cell lines we observed a very potent knockdown of EZH2 and moderately reduced H3K27me3 levels. Strikingly, in Karpas-422 cells we found a very strong decrease of the H3K27 monomethylation level as compared to the control, highlighting the importance of the wild type EZH2 for monomethylation of H3K27. The changes in di- and tri-methylation were not as drastic. This suggests probably the need to examine the methylation state of single EZH2 target promoters by chromatin-immunoprecipitation (ChIP) approaches rather than analyzing the global methylation levels by Western blot as performed in our studies.

Remarkably, the androgen sensitive prostate cell line LNCaP.FGC showed a potent inhibition of cell proliferation upon EZH2 knockdown as shown in Figure 27. The PC3 cells express the lowest amount of EZH2 protein of all cell lines tested in our Western blot analysis (Figure 14). It seems that they are not dependent on EZH2 for cell proliferation in two dimensional cell proliferation assays (see Figure 25). We also knocked down EZH2 in another androgen insensitive prostate cancer cell line, the DU-145, but could not obtain conclusive results (data not shown). Future studies should be aimed at testing the effect of EZH2 knockdown in these cells using cell invasion assays or soft agar colony formation assays, which mimic more closely the environment tumor cells encounter in vivo. More prostate cancer cell lines, androgen dependent as well as androgen insensitive, should be tested to gain further insights into the mechanisms of EZH2 regulation.

The knockdown of EZH2 in various cell lines in all cases led to a reduction of global H3K27 trimethylation levels. Although in some cases the reduction in trimethylation levels on a global scale did not seem to be very extensive, on the single gene level there could possibly be stronger differences.

For this reason we selected 10 published EZH2 target genes and tested the response on target gene expression upon EZH2 knockdown by RT q-PCR. As expected, we observed very different results in different cell lines. MiaPaCa-2 cells upregulated several genes among which TXNIP was increased 10-fold. The tumor suppressor TXNIP, a key regulator

of the redox system, negatively regulates thioredoxin (TRX) and has strong growth suppressive, metastasis inhibitory and proapoptotic function [69]. The TXNIP gene is highly conserved from zebrafish to humans and is often suppressed in human cancers by mechanisms other than deletion, translocation or somatic mutation [69]. TXNIP directly binds to TRX and thereby inhibits its function as an important molecule for redox control. This excessively increases reactive oxygen species (ROS) leading to apoptosis via the endoplasmatic reticulum (ER) stress response [68]. The role of EZH2 in modulating ER stress response might be a new mechanism for its oncogenic function. Future studies should be aimed at clarifying this.

Among the upregulated genes following EZH2 knockdown, we also found EED and SUZ-12, members of the PRC2. EZH2 probably plays a role in auto-regulation of the complex as reported previously for members of PRC1 [1]. In MiaPaCa-2 cells we observed upregulation of EZH1. This could either be a mechanism to compensate for the loss of EZH2 and keep up target gene repression, or be part of a cellular mechanism to switch from a proliferative to a differentiated state. Consistent with this, EZH1 has been reported as a key enzyme which induces molecular pathways leading to cell differentiation [70]. While EZH2 is mainly found in undifferentiated, proliferating cells, EZH1 is expressed in non-proliferative adult organs [22] and during differentiation EZH2 is replaced by EZH1 at certain target genes [70]. Further studies should define if EZH1 has a redundant role to EZH2 in tumorigenesis. This is essential in the process of developing an EZH2 inhibitor. In case of redundancy the inhibitor can target both proteins, in case of differential roles it would be more beneficial for cancer patients the administration of a selective inhibitor. In MiaPaCa-2 cells there seems to be a compensatory mechanisms of EZH1 which we could not observe in most other cell lines. Double knockdown experiments targeting both EZH1 and EZH2 for knockdown simultaneously could help in clarifying this issue.

An EZH2 inhibitor could target the catalytically active SET domain, because it is structurally well conserved. The SET protein family contains about fifty proteins in humans [71]. If no specific inhibitor of the SET domain could be identified, another

possibility might be to target the interaction of EZH2 with EED and/or SUZ12, which abolishes the methyltransferase function.

The importance of EZH2 for tumor cell proliferation could be further validated by rescue experiments. The re-introduction of a shRNA-insensitive form of EZH2 in EZH2 knockdown cells would be an intriguing approach to demonstrate the dependency of cells on the enzymatic function of this enzyme. Nevertheless any changes in epigenetic states of cells take some cell divisions to fully take effect and the evaluation of these outcomes might be quite challenging. Reintroducing EZH2 into cells in which the protein has been knocked down might not reconstitute the initial transcriptional state of the cells due to the complex regulatory networks EZH2 is part of.

One of the major pitfalls in drug discovery today is the low percent of success of a drug during the drug development process. This mostly happens because during clinical trials the responsive patient population is often poorly defined. The knockdown experiments we carried out might help in the identification of the patient population that could be targeted by an EZH2 inhibitor. We demonstrated that cells with EZH2 amplification, EZH2 point mutation and UTX deletion show reduced cell proliferation upon EZH2 knockdown, while cells merely overexpressing EZH2 by undefined mechanisms do not respond as clearly.

SUMMARY

The histone methyltransferase EZH2 has been implicated in cancer cell proliferation and associated with late stage aggressive tumors by repressive hypertrimethylation of H3K27. It is involved in the repression of differentiation genes, rendering the tumors in a highly proliferative, undifferentiated state. We showed that knockdown of EZH2 reduces the proliferation of a broad panel of tumor cell lines.

We knocked down EZH2 by shRNA in cell lines with various backgrounds of aberrant EZH2 expression. We found significantly reduced proliferation in EZH2 amplified cells and cells with a deletion of the H3K27 demethylase UTX. In B-cell lymphoma cells with a heterozygous mutation that increases di- and tri-methylation activity of EZH2 we could observe a significant decrease in proliferation upon EZH2 knockdown. EZH2 overexpressing cells responded in a less pronounced way. In prostate cancer we found an androgen dependent cell line highly susceptible to EZH2 knockdown, while an androgen insensitive cell line did not respond in 2D proliferation assays. EZH2 knockdown was in all cases associated with a global decrease of the H3K27 trimethylation mark. Analysis of target gene mRNA expression changes upon EZH2 knockdown revealed reactivation of tumor suppressors in several cell lines tested. EZH2 is therefore a promising target in cancer treatment, as it is expressed mainly in highly proliferative tumor cells and not in differentiated adult tissues. Also epigenetic effects are reversible; changes caused by drugs targeting an epigenetic target could be reverted after successful anti cancer therapy.

REFERENCES

1. Bracken, A.P., et al., *Genome-wide mapping of Polycomb target genes unravels their roles in cell fate transitions.* Genes Dev, 2006. **20**(9): p. 1123-36.
2. Schones, D.E. and K. Zhao, *Genome-wide approaches to studying chromatin modifications.* Nat Rev Genet, 2008. **9**(3): p. 179-91.
3. Martens, J.H., H.G. Stunnenberg, and C. Logie, *The decade of the epigenomes?* Genes Cancer, 2011. **2**(6): p. 680-7.
4. Jeronimo, C., et al., *Epigenetics in prostate cancer: biologic and clinical relevance.* Eur Urol, 2011. **60**(4): p. 753-66.
5. Alberts, B., et al., eds. *Molecular Biology Of The Cell, 4th edition*. 4th edition ed. 2002, Garland Science: New York, NY 10016.
6. Rajasekhar, V.K. and M. Begemann, *Concise review: roles of polycomb group proteins in development and disease: a stem cell perspective.* Stem Cells, 2007. **25**(10): p. 2498-510.
7. Islam, A.B., et al., *Selective targeting of histone methylation.* Cell Cycle, 2011. **10**(3): p. 413-24.
8. Munshi, A., et al., *Histone modifications dictate specific biological readouts.* J Genet Genomics, 2009. **36**(2): p. 75-88.
9. Kuzmichev, A., et al., *Different EZH2-containing complexes target methylation of histone H1 or nucleosomal histone H3.* Mol Cell, 2004. **14**(2): p. 183-93.
10. Barski, A., et al., *High-resolution profiling of histone methylations in the human genome.* Cell, 2007. **129**(4): p. 823-37.
11. Jones, P.A. and S.B. Baylin, *The epigenomics of cancer.* Cell, 2007. **128**(4): p. 683-92.
12. van Haaften, G., et al., *Somatic mutations of the histone H3K27 demethylase gene UTX in human cancer.* Nat Genet, 2009. **41**(5): p. 521-3.
13. Simon, J.A. and C.A. Lange, *Roles of the EZH2 histone methyltransferase in cancer epigenetics.* Mutat Res, 2008. **647**(1-2): p. 21-9.
14. Chou, R.H., Y.L. Yu, and M.C. Hung, *The roles of EZH2 in cell lineage commitment.* Am J Transl Res, 2011. **3**(3): p. 243-50.
15. Laible, G., et al., *Mammalian homologues of the Polycomb-group gene Enhancer of zeste mediate gene silencing in Drosophila heterochromatin and at S. cerevisiae telomeres.* Embo J, 1997. **16**(11): p. 3219-32.
16. Kuzmichev, A., et al., *Histone methyltransferase activity associated with a human multiprotein complex containing the Enhancer of Zeste protein.* Genes Dev, 2002. **16**(22): p. 2893-905.
17. Muller, J., et al., *Histone methyltransferase activity of a Drosophila Polycomb group repressor complex.* Cell, 2002. **111**(2): p. 197-208.
18. Xu, C., et al., *Binding of different histone marks differentially regulates the activity and specificity of polycomb repressive complex 2 (PRC2).* Proc Natl Acad Sci U S A, 2010. **107**(45): p. 19266-71.
19. Pasini, D., et al., *Suz12 is essential for mouse development and for EZH2 histone methyltransferase activity.* Embo J, 2004. **23**(20): p. 4061-71.

20. Ringrose, L. and R. Paro, *Epigenetic regulation of cellular memory by the Polycomb and Trithorax group proteins.* Annu Rev Genet, 2004. **38**: p. 413-43.
21. Richly, H., L. Aloia, and L. Di Croce, *Roles of the Polycomb group proteins in stem cells and cancer.* Cell Death Dis, 2011. **2**: p. e204.
22. Margueron, R., et al., *Ezh1 and Ezh2 maintain repressive chromatin through different mechanisms.* Mol Cell, 2008. **32**(4): p. 503-18.
23. Abel, K.J., et al., *Characterization of EZH1, a human homolog of Drosophila Enhancer of zeste near BRCA1.* Genomics, 1996. **37**(2): p. 161-71.
24. Shen, X., et al., *EZH1 mediates methylation on histone H3 lysine 27 and complements EZH2 in maintaining stem cell identity and executing pluripotency.* Mol Cell, 2008. **32**(4): p. 491-502.
25. Ezhkova, E., et al., *EZH1 and EZH2 cogovern histone H3K27 trimethylation and are essential for hair follicle homeostasis and wound repair.* Genes Dev, 2011. **25**(5): p. 485-98.
26. Caretti, G., et al., *The Polycomb Ezh2 methyltransferase regulates muscle gene expression and skeletal muscle differentiation.* Genes Dev, 2004. **18**(21): p. 2627-38.
27. Tong, Z.T., et al., *EZH2 supports nasopharyngeal carcinoma cell aggressiveness by forming a co-repressor complex with HDAC1/HDAC2 and Snail to inhibit E-cadherin.* Oncogene, 2011.
28. Bracken, A.P., et al., *EZH2 is downstream of the pRB-E2F pathway, essential for proliferation and amplified in cancer.* Embo J, 2003. **22**(20): p. 5323-35.
29. Shaw, T. and P. Martin, *Epigenetic reprogramming during wound healing: loss of polycomb-mediated silencing may enable upregulation of repair genes.* EMBO Rep, 2009. **10**(8): p. 881-6.
30. Varambally, S., et al., *Genomic loss of microRNA-101 leads to overexpression of histone methyltransferase EZH2 in cancer.* Science, 2008. **322**(5908): p. 1695-9.
31. Cao, Q., et al., *Coordinated Regulation of Polycomb Group Complexes through microRNAs in Cancer.* Cancer Cell, 2011. **20**(2): p. 187-99.
32. Cao, P., et al., *MicroRNA-101 negatively regulates Ezh2 and its expression is modulated by androgen receptor and HIF-1alpha/HIF-1beta.* Mol Cancer, 2010. **9**: p. 108.
33. Nakahara, O., et al., *Carcinogenesis of Intraductal Papillary Mucinous Neoplasm of the Pancreas: Loss of MicroRNA-101 Promotes Overexpression of Histone Methyltransferase EZH2.* Ann Surg Oncol, 2011.
34. Caretti, G., et al., *Phosphoryl-EZH-ion.* Cell Stem Cell, 2011. **8**(3): p. 262-5.
35. Kaneko, S., et al., *Phosphorylation of the PRC2 component Ezh2 is cell cycle-regulated and up-regulates its binding to ncRNA.* Genes Dev, 2010. **24**(23): p. 2615-20.
36. Tsai, M.C., et al., *Long noncoding RNA as modular scaffold of histone modification complexes.* Science, 2010. **329**(5992): p. 689-93.
37. Zhao, J., et al., *Polycomb proteins targeted by a short repeat RNA to the mouse X chromosome.* Science, 2008. **322**(5902): p. 750-6.
38. Lee, T.I., et al., *Control of developmental regulators by Polycomb in human embryonic stem cells.* Cell, 2006. **125**(2): p. 301-13.

39. Boyer, L.A., et al., *Polycomb complexes repress developmental regulators in murine embryonic stem cells.* Nature, 2006. **441**(7091): p. 349-53.
40. Ringrose, L., *Polycomb comes of age: genome-wide profiling of target sites.* Curr Opin Cell Biol, 2007. **19**(3): p. 290-7.
41. Juan, A.H., et al., *Polycomb EZH2 controls self-renewal and safeguards the transcriptional identity of skeletal muscle stem cells.* Genes Dev, 2011. **25**(8): p. 789-94.
42. Pardal, R., M.F. Clarke, and S.J. Morrison, *Applying the principles of stem-cell biology to cancer.* Nat Rev Cancer, 2003. **3**(12): p. 895-902.
43. Crea, F., et al., *Pharmacologic disruption of Polycomb Repressive Complex 2 inhibits tumorigenicity and tumor progression in prostate cancer.* Mol Cancer, 2011. **10**: p. 40.
44. Bachmann, I.M., et al., *EZH2 expression is associated with high proliferation rate and aggressive tumor subgroups in cutaneous melanoma and cancers of the endometrium, prostate, and breast.* J Clin Oncol, 2006. **24**(2): p. 268-73.
45. Varambally, S., et al., *The polycomb group protein EZH2 is involved in progression of prostate cancer.* Nature, 2002. **419**(6907): p. 624-9.
46. Yu, J., et al., *A polycomb repression signature in metastatic prostate cancer predicts cancer outcome.* Cancer Res, 2007. **67**(22): p. 10657-63.
47. Takawa, M., et al., *Validation of the histone methyltransferase EZH2 as a therapeutic target for various types of human cancer and as a prognostic marker.* Cancer Sci, 2011. **102**(7): p. 1298-305.
48. Fussbroich, B., et al., *EZH2 depletion blocks the proliferation of colon cancer cells.* PLoS One, 2011. **6**(7): p. e21651.
49. Karanikolas, B.D., M.L. Figueiredo, and L. Wu, *Comprehensive evaluation of the role of EZH2 in the growth, invasion, and aggression of a panel of prostate cancer cell lines.* Prostate, 2010. **70**(6): p. 675-88.
50. Gonzalez, M.E., et al., *Downregulation of EZH2 decreases growth of estrogen receptor-negative invasive breast carcinoma and requires BRCA1.* Oncogene, 2009. **28**(6): p. 843-53.
51. Kleer, C.G., et al., *EZH2 is a marker of aggressive breast cancer and promotes neoplastic transformation of breast epithelial cells.* Proc Natl Acad Sci U S A, 2003. **100**(20): p. 11606-11.
52. Lee, S.T., et al., *Context-Specific Regulation of NF-kappaB Target Gene Expression by EZH2 in Breast Cancers.* Mol Cell, 2011. **43**(5): p. 798-810.
53. Morin, R.D., et al., *Somatic mutations altering EZH2 (Tyr641) in follicular and diffuse large B-cell lymphomas of germinal-center origin.* Nat Genet, 2010. **42**(2): p. 181-5.
54. Sneeringer, C.J., et al., *Coordinated activities of wild-type plus mutant EZH2 drive tumor-associated hypertrimethylation of lysine 27 on histone H3 (H3K27) in human B-cell lymphomas.* Proc Natl Acad Sci U S A, 2010. **107**(49): p. 20980-5.
55. Parisi, F., et al., *Detecting copy number status and uncovering subclonal markers in heterogeneous tumor biopsies.* BMC Genomics, 2011. **12**: p. 230.
56. Darken, M.A., *Puromycin Inhibition of Protein Synthesis.* Pharmacol Rev, 1964. **16**: p. 223-43.

57. Yarmolinsky, M.B. and G.L. Haba, *Inhibition by Puromycin of Amino Acid Incorporation into Protein.* Proc Natl Acad Sci U S A, 1959. **45**(12): p. 1721-9.
58. Perez-Gonzalez, J.A., J. Vara, and A. Jimenez, *The mechanism of resistance to puromycin and to the puromycin-precursor O-demethyl-puromycin in Streptomyces alboniger.* J Gen Microbiol, 1985. **131**(11): p. 2877-83.
59. O'Doherty, U., W.J. Swiggard, and M.H. Malim, *Human immunodeficiency virus type 1 spinoculation enhances infection through virus binding.* J Virol, 2000. **74**(21): p. 10074-80.
60. Livak, K.J. and T.D. Schmittgen, *Analysis of relative gene expression data using real-time quantitative PCR and the 2(-Delta Delta C(T)) Method.* Methods, 2001. **25**(4): p. 402-8.
61. Tsang, D.P. and A.S. Cheng, *Epigenetic regulation of signaling pathways in cancer: role of the histone methyltransferase EZH2.* J Gastroenterol Hepatol, 2010. **26**(1): p. 19-27.
62. Fan, T., et al., *EZH2-dependent suppression of a cellular senescence phenotype in melanoma cells by inhibition of p21/CDKN1A expression.* Mol Cancer Res, 2011. **9**(4): p. 418-29.
63. Kheradmand Kia, S., et al., *EZH2-dependent chromatin looping controls INK4a and INK4b, but not ARF, during human progenitor cell differentiation and cellular senescence.* Epigenetics Chromatin, 2009. **2**(1): p. 16.
64. Cao, Q., et al., *Repression of E-cadherin by the polycomb group protein EZH2 in cancer.* Oncogene, 2008. **27**(58): p. 7274-84.
65. Wang, C., et al., *Polycomb group protein EZH2-mediated E-cadherin repression promotes metastasis of oral tongue squamous cell carcinoma.* Mol Carcinog, 2011.
66. Min, J., et al., *An oncogene-tumor suppressor cascade drives metastatic prostate cancer by coordinately activating Ras and nuclear factor-kappaB.* Nat Med, 2010. **16**(3): p. 286-94.
67. Du, J., et al., *FOXC1, a target of polycomb, inhibits metastasis of breast cancer cells.* Breast Cancer Res Treat, 2011. **131**(1): p. 65-73.
68. Zhou, J., et al., *The histone methyltransferase inhibitor, DZNep, up-regulates TXNIP, increases ROS production, and targets leukemia cells in AML.* Blood, 2011. **118**(10): p. 2830-9.
69. Zhou, J., Q. Yu, and W.J. Chng, *TXNIP (VDUP-1, TBP-2): a major redox regulator commonly suppressed in cancer by epigenetic mechanisms.* Int J Biochem Cell Biol, 2011. **43**(12): p. 1668-73.
70. Stojic, L., et al., *Chromatin regulated interchange between polycomb repressive complex 2 (PRC2)-Ezh2 and PRC2-Ezh1 complexes controls myogenin activation in skeletal muscle cells.* Epigenetics Chromatin, 2011. **4**: p. 16.
71. Schapira, M., *Structural Chemistry of Human SET Domain Protein Methyltransferases.* Curr Chem Genomics, 2011. **5**(Suppl 1): p. 85-94.

List of figures

Figure 1. Correlation of Histone Methylations in Transcribed Regions with Expression Levels. [10]. 10
Figure 2. Modified from poster presented at AACR 2010. Readers and writers adding and removing methyl-groups at lysines of Histone H3.. 11
Figure 3. Composition of PRC2 and domain organization of EZH2. [13] 13
Figure 4. Schematic model of epigenetic changes in the onset of cancer. [6]. 18
Figure 5. The refined 14 “Polycomb Repression Signature” genes proposed by Yu and colleagues. [46]. 19
Figure 6. PRC2 complexes containing mutant EZH2 preferentially catalyze di- and trimethylation of histone H3K27. [54]. 21
Figure 7. Proposed mechanisms leading to aberrantly high levels of trimethylation on histone H3K27 in cancer [54]. 22
Figure 8. Illustration of MISSION® shRNA Lentiviral Transduction Particles (http://www.sigmaaldrich.com/catalog/ProductDetail.do?lang=de&N4=SHC002H|SIGMA&N5=SEARCH_CONCAT_PNO|BRAND_KEY&F=SPEC; 06.12.11). 28
Figure 9. Lentiviral protein knockdown: experiment overview....29
Figure 10. Daily CSI proliferation measurement based on cell confluence. 32
Figure 11. Relative EZH2 expression levels in normal and cancer tissues. 43
Figure 12. Relative expression levels of EZH2 and EZH1 in a panel of human cancer cell lines.. 44
Figure 13. Amplification of EZH2 in C32 cells. 44
Figure 14. Verification of EZH2 protein expression levels by Western blot. 45
Figure 15. Knockdown of EZH2 by siRNA. 46
Figure 16. Validation of shRNA lentiviruses....48
Figure 17. Reduced proliferation in EVSA-T breast cancer cells dependent on cell number....50
Figure 18. Confirmation of EZH2 knockdown in EVSA-T breast cancer cells. 51
Figure 19. Reduced metabolic activity in cells with an EZH2 point mutation. 52
Figure 20. Verification of EZH2 knockdown in B-cell lymphoma cells....53

Figure 21. Reduced proliferation in C-32 melanoma cells with an EZH2 amplification of 3.8. 54
Figure 22. Western Blot analysis of EZH2 knockdown and H3K27 methylation status in C-32 cells 55
Figure 23. Reduced proliferation in UTX deleted MiaPaCa-2 Pancreas carcinoma cells .. 55
Figure 24. Verification of EZH2 knockdown in MiaPaCa-2 cells 56
Figure 25. Unchanged proliferation of PC3 prostate cancer cells after lentiviral knockdown of EZH2.. 57
Figure 26. Verification of EZH2 knockdown in PC3 androgen insensitive prostate carcinoma cells..... 58
Figure 27. Proliferation arrest of LNCaP.FGC androgen sensitive prostate cancer cells upon EZH2 knockdown. 58
Figure 28. Verification of EZH2 knockdown in LNCaP.FGC prostate carcinoma cells. 59
Figure 29. Reduced capacity to form colonies in soft agar of MiaPaCa-2 cells. 60
Figure 30. EZH2 target gene signature in MiaPaCa-2 cells (200c/w) and EVSA-T cells (800c/w). 62

List of tables

Table 1. List of cell lines 25
Table 2. Cell Culture Media 27
Table 3. Chemicals for Cell Culture 27
Table 4. Materials for shRNA transduction 29
Table 5. Sigma MISSION anti EZH2 Lentiviruses 29
Table 6. Cell detection methods used in the CSI cell proliferation assay. 32
Table 7. Materials for the metabolic Alamar Blue cell proliferation assay 33
Table 8. Materials for the soft agar colony formation assay 34
Table 9. Materials for whole cell lysates 35
Table 10. Materials for Bradford Protein concentration determination 36
Table 11. Materials for SDS Page 36

Table 12. Materials for Western Blot 37
Table 13. List of Antibodies used for Western Blot 38
Table 14. Materials for siRNA transfection.....39
Table 15. Materials for cDNA synthesis.....40
Table 16. Materials for RT q-PCR 41
Table 17. TaqManR Gene Expression Assays, Applied Biosystems 41
Table 18. List of cell lines used for knockdown experiments. 44
Table 19. Optimal puromycin concentrations determined for different cancer cell lines.
.....47
Table 20. List of genes analyzed in RT q-PCR gene signature experiments.....61

Ich habe mich bemüht, sämtliche Inhaber der Bildrechte ausfindig zu machen und ihre Zustimmung zur Verwendung der Bilder in dieser Arbeit eingeholt. Sollte dennoch eine Urheberrechtsverletzung bekannt werden, ersuche ich um Meldung bei mir.

Curriculum Vitae

Personal information	
First name / Surname	**Renner Magdalena**
Address	Alserbachstraße 35/9, 1090 Wien, Austria
E-mail	a0606472@unet.univie.ac.at
Nationality	Austria
Date of birth	02.09.1987
Education	
March - December 2011	**Diploma Thesis Research** at Boehringer Ingelheim GmbH & CoKG Vienna, Austria
February – June **2010**	**ERASMUS exchange semester** in Brussels, Belgium at the „Vrije Universiteit Brussel“ Undertook university modules in “Cell and gene Therapy”, with two months of laboratory internship
November 2009	Commencement of second half of diploma studies, equivalent to a master degree Study focuses: - Molecular Medicine - Biochemistry - Immunology
November 2009	Completion of the first half of diploma studies, equivalent to a bachelor degree
October 2006	**Initiation of diploma studies “Molecular Biology” at the University of Vienna, Austria**
June 2006	**Graduation with distinction**
1998-2006	Bundesgymnasium Vöcklabruck (Secondary academic school)
1994-1998	Volksschule Attnang-Puchheim (Primary School)
Training and work experience	

March 2011 until present	**Research work on Diploma Thesis**
Laboratory	Group of Davide Gianni Lead Discovery at Boehringer Ingelheim GmbH & CoKG Vienna, Austria
Title of Thesis	Study of the function of the histone methyltransferase EZH2 in human cancers
January – February 2011	**Laboratory internship in the field of micro RNA (1 month)**
Laboratory	Group of Silke Dorner Max F. Perutz Laboratories Vienna
Title of project	Purification of three protein fragments of proteins involved in the drosophila miRNA degradation pathway
November – December 2010	**Laboratory internship in the field of nuclear lamins (1 month)**
Laboratory	Group of Roland Foisner Max F. Perutz Laboratories Vienna
Title of project	The role of Lap2α in regulating the nucleoplasmic Lamin A/C pool
September – November 2010	**Laboratory internship in the field of allergy research (2 months)**
Laboratory	Group of Rudolf Valenta Center for Physiology and Pathophysiology, Medical University of Vienna
Title of project	Analysis of a hypoallergenic parvalbumin mutant for treatment of fish allergy
February – March 2010	**Laboratory internship in the field of multiple sclerosis (2 months)**
Laboratory	Group of Ralph Clinckers Institute of Pharmaceutical Chemistry at the Vrije Universiteit Brussel
Title of project	The role of astrocytic β2 adrenoreceptor in the pathophysiology of multiple sclerosis
September – October 2009	**Laboratory internship in the field of RNA research (1 month)**
Laboratory	Group of Christina Waldsich Max F. Perutz Laboratories Vienna
Title of project	Splicing activity of introns in yeast mitochondria
July 2008	**Laboratory technician (1 month)**
Laboratory	Blood Bank of the Red Cross Linz, Austria
August – September 2007	**Vacation work** office of Dr. Johann Renner, medical practitioner in Attnang-Puchheim, Austria